A survey on tracking control of unmanned underwater vehicles: Experiments-based approach

Auwal Tijjani Shehu, Ahmed Chemori, Vincent Creuze

A Survey on Tracking Control of Unmanned Underwater Vehicles: Experiments-Based Approach

Auwal Shehu Tijjani[a], Ahmed Chemori,[a,*] and Vincent Creuze[a]

[a]LIRMM, University of Montpellier, CNRS, Montpellier, France

ARTICLE INFO

Keywords:
Unmanned underwater vehicles (UUVs)
Trajectory tracking
Adaptive control
Combined control
Sliding mode control (SMC)
Observation-based control
Real-time experiments.

ABSTRACT

This paper aims to provide a review of the conceptual design and theoretical framework of the main control schemes proposed in the literature for unmanned underwater vehicles (UUVs). Additionally, the objective of the paper is not only to present an overview of the recent control architectures validated on UUVs but also to give detailed experimental-based comparative studies of the proposed control schemes. To this end, the main control schemes, including proportional-integral-derivative (PID) based, sliding mode control (SMC) based, adaptive based, observation-based, model predictive control (MPC) based, combined control techniques, are revisited in order to consolidate the principal efforts made in the last two decades by the automatic control community in the field. Besides implementing some key tracking control schemes from the classification mentioned above on *Leonard UUV*, several real-time experimental scenarios are tested, under different operating conditions, to evaluate and compare the efficiency of the selected tracking control schemes. Furthermore, we point out potential investigation gaps and future research trends at the end of this survey.

1. Introduction and related work

1.1. Context

The marine/underwater environments pose technical, scientific, and economic challenges in accessing most of their deeper floors Chen et al. (2018), Bibuli and Zereik (2018). Despite these environments covering approximately 71 % of the earth as well as supporting approximately 90 % of the life forms, the issues, mentioned above, associated with the environments make them highly unknown to humans Yang et al. (2021b). Therefore, exploration and exploitation of the underwater in a sustainable approach should result in huge benefits from various resources of the environments Vu et al. (2021), which are vital for enhancing the quality of human life. To have access to the resources of this strategic and resource-based environment, all its problems need to be faced with sophisticated and cutting-edge technologies, such as using intelligent systems Hu et al. (2020). Indeed, these systems will help in exploring the majority of the underwater environments, which remain presently unknown to humans. Even though several attempts have been made to access some areas, especially deeper regions, of the underwater environments using divers as well as manned submersibles (e.g. submarines), these conventional methods present significant safety issues to both the vehicles and the humans during deep-underwater missions. One of the main reasons for the inaccessible nature of the deeper sides of the underwater environments lies mainly in the hash geographical characteristics of the regions, which include poor visibility, extreme pressure, low temperature, high depth, unstructured terrain, etc. Jaffe et al. (2017), Zhang et al. (2021). All these challenges emphasize the necessity of fully autonomous systems equipped with cutting-edge/intelligent capabilities to explore and exploit underwater environments Simetti et al. (2021a).

In view of the above-mentioned requirement, many research communities in the domain of robotics proposed deploying robots to explore and exploit the underwater environment. This leads to the evolution of a new era of robots called unmanned underwater vehicles/robots (UUVs) Yang et al. (2021a). Consequently, the discovery and exploitation of deep-oceans/seas areas in addition to the activities of maritime industries have recorded significant progress for the last two decades Heshmati-Alamdari et al. (2021). This success has been mainly achieved in the robotic community due to the effectiveness, reliability, and flexibility demonstrated by UUVs in helping humans to execute several underwater operations successfully. Moreover, these kinds of vehicles have the capacity to extend some of the intelligent actions of a human to highly unknown and unstructured underwater environments. In line with this philosophy, UUVs have been used predominantly in a variety of underwater applications Teeneti et al. (2021). Some of the applications of the UUVs include inspection and maintenance of marine structures, scientific investigation of marine environments/environs and their ecosystems, exploration and exploitation of subsea mineral deposits, surveillance and control of maritime borders, mine countermeasures, etc. Tijjani et al. (2021), Li et al. (2017). Based on these fascinating applications and more of the UUVs, in addition to their capabilities to operate in other sensitive undersea environments like iced regions Caharija et al. (2016), they have motivated a vast number of interdisciplinary research works aiming to investigate as well as efficiently utilize the subsea Nađ et al. (2015). Furthermore, executing underwater operations using UUVs are cost-effective and safer when compared to the traditional techniques, where divers or submarines are deployed.

*Corresponding author

atshehu@lirmm.fr (A.S. Tijjani); ahmed.chemori@lirmm.fr (A. Chemori,); vincent.creuze@lirmm.fr (V. Creuze)

ORCID(s):

In spite of all the success and the advancement in the UUVs technology, several problems are faced during day-to-day underwater missions using the vehicles Kong et al. (2021). For instance, UUVs face many challenges in terms of communications, robust perception and sensing, reliable autonomy, etc. A reliable autonomous control scheme design is one of the persisting issues concerning autonomous vehicles' technology in general, including UUVs as pointed out by Antsaklis (2020). It is worth noting that various marine operations, like high-quality deep-sea surveys Noguchi and Maki (2021), are possible through one or combination of motion scenarios such as high precision path following, target tracking, dynamic positioning, and trajectory tracking of the vehicles Kumar et al. (2007), Peng et al. (2021). Hence, it is essential to design a high precision control scheme that can autonomously guide these vehicles for successful marine tasks. However, unlike the autonomous systems prevalent in-air and structured environments, this new wave of autonomous systems (or UUVs) are operating in highly unknown and unstructured environments, where the UUVs depend only on their onboard sensors, computational algorithms, and actuators. Furthermore, the hydrodynamics effects, ocean loads (e.g. currents and waves), and coupled system's states complicate the behavior of UUVs Liu et al. (2021a). For all these reasons, the vehicles are characterized by highly complex dynamics Batmani and Najafi (2021); Liu et al. (2017). Thus, the control system design for such vehicles becomes one of the most critical parts when building new UUVs Yan and Yu (2018). Although one can notice significant advancement in terms of UUVs control technology from the literature Boehm et al. (2021), still designing reliable autonomous control algorithms for UUVs to track a predefined trajectory remains a nontrivial task Seok Park (2015).

1.2. Motivation

The roles played by UUVs, in dealing with many challenges faced in various interdisciplinary fields, when exploring and exploiting marine/underwater environments motivated this survey. Apart from protecting and saving humans' lives in many underwater operations, the UUVs are essential in providing genuine/accurate information of a vast number of maritime incidences beyond human control. Furthermore, the uncertainties and the low efficiency of manned submersibles, in different marine applications such as maritime borders defence, lead to the increasing interest in UUVs research nowadays. Some of the major problems of submarines include (i) getting stuck in a confined deep-ocean/sea area, (ii) communication lost between the submarine and its based-station, etc. All these issues may result in putting the lives of the submarine crew members at risk. Examples of real-life scenarios reaffirming the reliability of UUVs in critical marine situations include:

- A submarine, which is identified as AS-28, was trapped by radar cables at an approximately 250 m depth in front of the *Kamchatka, Russia* Antonelli (2014). Many strategies have been deployed to rescue the submarine without achieving any success. However, a UUV named *Scorpio* successfully cuts the cables within 24 hours; as a result, all the seven crew members inside the vehicle have been rescued alive. Moreover, the submarine has been recovered in good condition during the operation.
- Recently, a 44-year-old $Nanggala$-402 submarine disappeared with its 53 crew members. Even though the UUVs have been lately deployed during the tragedy, the vehicles are able to recover some of the wreckage of the submarine within a short time. The wreckage has been found at a depth of around 840 m off the coast of *Bali, Indonesia*. Unfortunately, all the crew members of the submarine are lost due to the fatal explosion of the submarine.

In line with these critical applications of UUVs and the issues faced by the manned submarines, the UUVs are dominating almost all the aspects of the marine operations up-to-the-minute Tijjani and Chemori (2020). Following this philosophy, the present survey is primarily motivated to progressively revisit the main research works dealing with the autonomy of UUVs. To emphasize more, the survey focuses specifically on the autonomous control schemes of low-cost versions of the UUVs. It is worth noting that the recent technological advances in microprocessors, control systems, light/high capacity battery systems, intelligent sensors and improved vision systems improve the autonomy of the UUVs.

1.3. Challenging Issues Faced in Real-Time Control

1.3.1. General case of robotic systems

Complex nonlinear dynamics: The intrinsic nonlinear behavior of most of robotic systems makes them extremely challenging to control. Besides having multiple-input multiple-output dynamics Liu et al. (2019a), the dynamics of these systems become more and more complex when following some specific tasks, such as intervention operations. Indeed, the kinematics of robotic systems poses a constraint as it is not always defined and invertible when represented using the well-known *Euler* angles notations. It is worth noting that the kinematics is a fundamental mathematical function utilized for 3-dimensional (3D) transformations between the reference frames in the control law design of robotic systems. Therefore, a constraint based robust nonlinear control scheme is needed to resolve this issue.

High parametric uncertainties: Another well-known issue concerning robotic systems is high internal (model) and external (operating environment) uncertainties McMahon and Plaku (2016). From the control point of view, the parameters' of these systems are often unknown and uncertain Xu et al. (2013). Even though various estimation techniques have been proposed from the literature, estimating the nominal parameters of the system with a certain accuracy still remain a long-lasting problem Avila et al. (2013), Gibson and Stilwell (2020).

Expensive cost of sensors and actuators: The high cost of accurate sensors and actuators is one of the financial constraints when designing a new robot Harris and Whitcomb (2021). This problem becomes more critical for the case of building a low-cost version of the robots to be deployed for special intervention missions Ji et al. (2021). In fact, some advanced sensors are not available at any cost Yuh (2000). Concerning the actuators, on the other hand, it is obvious that in a critical application, where the robots are subjected to high degree uncertainties and time-varying disturbances, high control efforts are required to compensate for such effects.

Inaccessible states: In practice, full-state measurements of the majority of the physical systems are often not available due to technical or economic constraints Baruch et al. (2020). Therefore, the classical solution to this issue is to design a state observer Zemouche et al. (2019). This approach has been used often to provide full-states as well as disturbances estimations to the control algorithms. Hence, observers have been a hot research topic, attracting the interest of industries to minimize the cost of the sensors.

Control design issues: Designing a control law for the robots is not a trivial task Saback et al. (2019). This problem is mainly caused by the complex nonlinear dynamics, high parametric uncertainties, and hardware constraints of the systems. Consequently, the design of an autonomous tracking control scheme for these systems becomes a long-lasting issue in robotics communities Yang et al. (2019).

1.3.2. Specific case of UUVs

Although UUVs are tools now widely used to operate in underwater environments, there are still various issues related the UUVs themselves. For example, compared to the general robotic systems previously discussed, the UUVs are characterized by the strong coupling effects between the vehicles' states Elmokadem et al. (2017). This effect becomes more and more pronounced for UUVs during marine operations such as intervention tasks. To minimize this effect by decoupling the states of the UUVs, as well as by taking into account kinematic constraints, many robust nonlinear MPC (NMPC) based controllers have been designed in the literature.

Furthermore, in some specific intervention operations, UUVs are constrained to a particular orientation w.r.t certain degrees of freedom (DOFs). For instance, a UUV equipped with a robotic manipulator can be constrained to move in four DOFs (i.e. three translational and one rotational) only while the remaining two DOFs like the roll (ϕ) and the pitch (θ) need to be stabilized around zero (i.e. $\phi \approx \theta \approx 0$) Campos et al. (2017). Many applications require the UUVs to fulfil the conditions above, otherwise, the vehicles' behavior may be considered not favorable for executing the tasks Zhou et al. (2020). Based on this requirement, taking into account the constraints in the design of a motion controller for the vehicles will improve its performance. In practice, some other constraints can be found at the input or the output of the vehicles Zhang and Wu (2021). To deal with this problem, MPC and MPC-based control schemes can be implemented on vehicles Yan et al. (2020b). For example, a robust NMPC has been developed specifically for UUVs in Heshmati-alamdari et al. (2019). Besides equipping the proposed control schemes with an obstacle avoiding behavior to improve the safety of the vehicles in any uncertain workspace, the proposed NMPC algorithm is computed online. Furthermore, the state feedback control law has been developed to ensure that the vehicles' trajectories stay and remain in a hyper-tube centered around the predefined desired trajectories. However, there is no evidence to confirm the effectiveness of the proposed control law for real-time missions.

Another key problem peculiar to UUVs is the disturbing effects of the sea (e.g. waves, currents, etc.) Ahn et al. (2010). For this reason, even the well-know adaptive control schemes may suffer a lot from the changes caused by these disturbances; furthermore, the hydrodynamic estimation tools are expensive, slow, and mostly not available to low-cost UUVs' designers Makavita et al. (2019). In addition, the mechanical actuators (fins, thrusters, and rudders) of these UUVs have limited bandwidth, which restricts the performance of the control algorithm implemented on such vehicles Li et al. (2021). Besides, some critical sensors such as a Doppler Velocity Log (DVL), used to provide velocity feedback for controlling the UUV, are not often installed on low-cost versions of the vehicles Meurer et al. (2020), Simetti et al. (2021b). Although the attitude and depth of the UUVs can easily be measured using any Inertial Measurement Unit (IMU) and pressure sensor, respectively Lin et al. (2020), it is almost impossible to configure these (only two) low-cost sensors to replace a costly DVL for measuring the linear velocity Zheng et al. (2020). To resolve all these problems, state estimation becomes necessary for the vehicles. Hence, a saturated observation-based control law can be considered as a potential solution. In line with this idea, different observer structures have been proposed in the literature (see Zemouche et al. (2019), Alessandri and Boem (2020), Wang et al. (2020a), for example).

Based on the above-mentioned issues concerning the control of UUVs, as well as the challenging nature of their operating environment combined with hardware constraints, many control methodologies have been proposed in the literature to resolve the UUVs' control problem (see for instance Campos et al. (2017), Guerrero et al. (2019a), Batmani and Najafi (2019), and Cui et al. (2019)). Following this philosophy, the present survey focuses only on the control solutions proposed for such vehicles. Additionally, special attention will be given to the controllers covering the low-cost versions of the vehicles. The forthcoming subsection discusses in depth the main control solutions attempting to deal with the problems highlighted, in this part, to improve the overall tracking control performance of the UUVs.

1.4. Main Existing Control Solutions for UUVs

Designing onboard controllers for UUVs based on the well-known linear techniques may lead to unacceptable performance. The performance of the control schemes is further degraded when the vehicles are operated in slightly different environmental settings. For this reason, an extensive number of research works have been conducted in marine robotics to resolve the control problems of UUVs, where the majority of these works aim to provide autonomous functionalities to the vehicles. These features are highly required for executing several real-time marine operations such as:

- *Path following*: This functionality can be described as a mission where the vehicles follow a spatial reference while executing a specific marine task.
- *Station keeping*: In marine robotics literature, this task is often called Dynamic Positioning "DP". The feature deals with keeping the UUVs at constants desired position and attitude during an underwater mission.
- *Spatial trajectory tracking*: Tracking is among the key functionalities highly essential for several marine applications, where the vehicles should track time-varying desired trajectories.

In order to be more clear, as well as to take into account some technical constraints, the following remark is necessary.

Remark 1. *even though we introduced three main control problems in marine robotics, including (i) path following, (ii) station keeping, and (iii) trajectory tracking, it is worth to emphasize that this paper is more focused on the third problem dealing with "Trajectory tracking". Indeed, the design of the representative controllers as well as their real-time experimental validations focus more on the trajectory tracking problem. The main reason why we focus on trajectory tracking problem is due to some technical issues, related to real-time experiments, we were faced with when considering the remaining problems. These technical issues include:*

- *The experimental setup at our disposal cannot enable us to conduct tests like path following. For instance, a large experimental testing pool is necessary for a typical path following test. As we only have a laboratory scale testing pool. Hence, this test is difficult to be conducted explicitly for our case.*
- *Another challenging issue is that our robot is not equipped with key sensors allowing us to perform station keeping tests (e.g. DVL). Consequently, this test is also difficult to be conducted in the experimental facilities at our disposal.*

On the other hand, observing carefully and technically the trajectory tracking we have conducted, in this paper, may be similar to a path following but with a limited number of DOFs, due to the limited number of sensors of equipping our robot. Furthermore, as we control simultaneously time-varying trajectories for two DOFs (representing one rotational motion and one translational motion), this could be easily extended to the case of a station-keeping problem.

In general, to equip the UUVs with the onboard control behaviors, mentioned previously, many control schemes have been proposed for such vehicles. We propose to classify the main existing ones from the literature with an illustrative overview, as shown in Fig. 1.

1.4.1. PD/PID control schemes

These control schemes are also called classical control laws, and they have been proposed to enhance the performance of conventional open-loop control techniques. Focusing on UUVs, these control methods are regarded as the most famous and common control laws used often to control the vehicles in the literature. From the practical point of view, the advantages of most of these control schemes are simple to design/implement as well as easy to tune online in real-time experiments Gan et al. (2020). The main reason is that their feedback gains can be easily selected, which lead to the stable behavior of their resulting closed-loop dynamics Sun and Cheah (2003). More precisely, a summary of the advantages of these schemes is given as follows:

- The control schemes can be implemented on physical vehicles or simulators without tears.
- The theoretical concepts of these control schemes are well-established. Furthermore, they are known to researchers and practitioners close to the control system communities with less expertise in the domain of automatic control.
- The feedback gains of the classical control schemes are mostly tuned by using the well-known trial-and-error techniques either online or offline.
- The well-established design tools and concepts used for linear systems can be exploited to facilitate the study of the linear approximations of their resulting closed-loop dynamics. This may resolve some of the complexities faced when analyzing the closed-loop dynamics.

Control schemes based on classical structures gained more place and much high ratings than advanced schemes. Following these advantages, PD/PID based control schemes are often used in the aspect of UUVs' control when compared to the advanced/complex control algorithms. For this reason, most of the laboratory-based and commercial off-the-shelf UUVs are controlled with these control schemes for many real-life marine operations Zhao and Guo (2020). We further subdivide classical control schemes into two major groups, as follows.

<u>*Non-model-based schemes:*</u> Control laws implemented on the UUVs utilizing only the information of the vehicles' states are named non-model-based control schemes Tijjani and Chemori (2021). Hence, these control schemes do not require any prior knowledge of the dynamics of the vehicle Liu et al. (2019b). Several control schemes based on classical structures have been proposed in the literature, which includes the following. A classical proportional integral

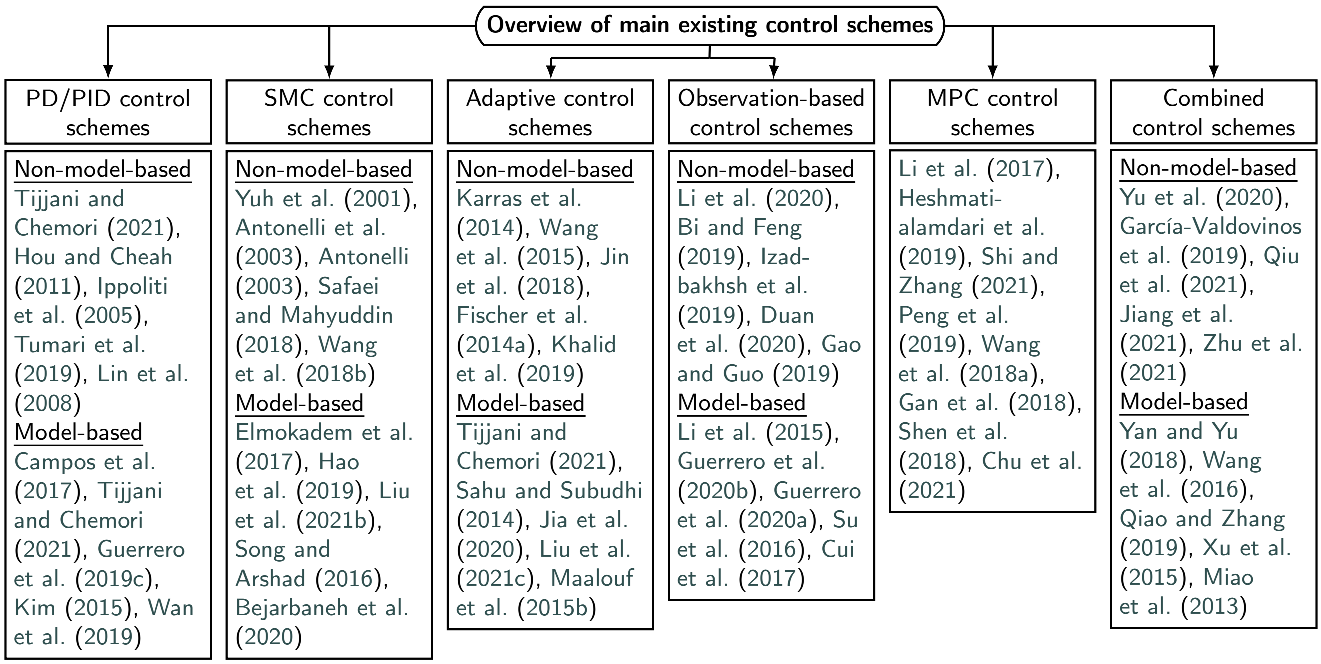

Figure 1: Overview of the main classes of existing onboard control schemes proposed for UUVs in the literature.

derivative (PID) scheme has been proposed to address the tracking control of six DOFs dynamics of an autonomous UUV in Tijjani and Chemori (2021). The control schemes based on the PID structure are among the well-known and widely applied control methods in practice Gan et al. (2020). Moreover, the PID control approach is often used as a benchmark to compare the performance of many advanced control techniques, especially for real-time applications. Considering the well-known acceptable performance of proportional derivative (PD) and PID control algorithms demonstrated in various industrial applications, an investigation has been conducted in Hou and Cheah (2011) and Hou and Cheah (2009) to explore the potentials of deploying these schemes for navigating multi-agent UUVs. These control schemes have been equipped with an obstacle/collision avoidance functionality using the multi-layer region concept. In spite of guaranteeing global asymptotic stability results in a systematic way, the performance of the PID-like control schemes is degraded when dealing with nonlinear coupled multiple-input multiple-output dynamics such as UUVs systems. Consequently, many improvement mechanisms have been integrated into the structures of the classical control schemes proposed in the literature, see for instance, a saturation-based nonlinear PID proposed in Guerrero et al. (2019c), a fuzzy logic-based PID developed in Geder et al. (2008), Hu et al. (2013), a GA-based PID designed in Chen et al. (2009), etc. Motivated by the unsatisfactory performance of conventional PID, an improved set-point tracking control has been developed using the concept of a supervision-based PID structure in Ippoliti et al. (2005). The design of three classical control schemes with different structures has been proposed in Smallwood and Whitcomb (2004) for UUVs. In order to further enhance the performance of the PID controller, optimization and intelligent mechanisms have been introduced into this control structure in Hernández-Alvarado et al. (2016) and Khodayari and Balochian (2015), respectively, to adjust its constant feedback gains online. This concept aims at improving/increasing the robustness of the control scheme based on the PID structure for marine applications. Following the same philosophy, an attempt has been made to design an alternative tuning technique for the conventional PID in Tumari et al. (2019). The improved PID control scheme has been validated through numerical simulations on a Hovering Autonomous Underwater Vehicle (HAUV) for a depth tracking control. One of the weaknesses of this study is that the evolution of the control signals has not been presented. Similarly, fuzzy-based PID and PD schemes have been designed for a low-cost UUV (called *U-FISH*) in Lin et al. (2008) and a high manoeuvred UUV in Londhe et al. (2017), respectively. It is worth noting that tuning a PID-like control scheme is a nontrivial task in the automatic control research community.

Model-based schemes: We can clearly observe that the improved non-model-based control schemes based on PD and PID structures always outperform the classical ones in most of the marine missions demonstrated using UUVs. Another idea proposed by many research communities to further improve the performances of the well-known PD/PID control schemes is adding more extra information concerning the vehicle's dynamics into the control algorithms. In general, this method always produces a remarkable result when the dynamics of the vehicles used in the control laws have some reasonable accuracy. For this reason, control schemes based on PD and PID structures have been extensively studied and implemented on UUVs in the literature; these research works include the following. In order to reaffirm the high ratings of model-based control schemes for real-time marine applications, an improved nonlinear PD+ (NLPD+) control architecture has been proposed in Campos et al. (2017). Besides adding the desired vehicle's dynamics in this control scheme, the authors proposed to replace the static feedback gains in the classical PD control law with saturation-based dynamic feedback gains. The saturation-based condition imposed on the gains mentioned previously has been relaxed in Campos et al. (2019); since the saturation function in the control scheme often limits the control inputs bandwidth when there is a high impact of disturbances/uncertainties. To enhance the robustness of the controller proposed in Campos et al. (2017) towards parametric uncertainties, a saturation based nonlinear PID (NLPID) has been developed and validated in Guerrero et al. (2019c). A model-based controller based on an exact linearization approach has been proposed in Smallwood and Whitcomb (2004) and Martin and Whitcomb (2013). The proposed control law has been deployed on the holonomic UUV (at Johns Hopkins University) and tested for six DOFs low-speed manoeuvring and station-keeping missions. This research work reinforces the superiority of the classical model-based controller (computed torque CT) over the traditional non-model-based PD control scheme for real-time marine applications. Besides conducting an experimental-based comparative study of the classical model-based and non-model-based controllers in Martin and Whitcomb (2012), a complete stability analysis for the control laws has been conducted. Additionally, a feedback linearizing control structure has been designed in Kim (2015) to deal with the tracking issues of autonomous UUVs. The well-known linear matrix inequalities (LMI) has been exploited, in this control scheme, to formulate the UUVs tracking control as an exponential stabilization problem of the vehicle's error dynamics. The main difference of the proposed control law compared to ones from the literature using the same LMI technique is that a nonlinear dynamics of UUV has been considered. Despite rigorous theoretical design in this work, the controller has been only validated using numerical examples. Furthermore, a cloud quantum-based algorithm has been proposed to compute the parameters of the fractional-order PID controller in Wan et al. (2019), aiming to improve the tracking control of the UUVs. Also, model-based nonlinear control schemes have been implemented on a biomimetic UUV (named *Aqua*) in Plamondon and Nahon (2008) in order to address the trajectory tracking problem of UUVs. All the proposed controllers have been validated through numerical simulations, followed by real-life experiments in the Caribbean Sea.

So far, the main objective of each control scheme, discussed, is to keep the vehicles around the desired trajectories as precisely as possible. Nevertheless, these control schemes are still affected by the sea loads. Even though adding the dynamics of the UUVs in the control architectures can significantly enhance the robustness of these controllers, obtaining a dynamic model representing the real vehicle with high accuracy is almost impossible due to hydrodynamic effects Zhu and Sun (2013). For all these issues, a well-known SMC-based (robust) control scheme may be the best technique to deal with the control problem of the UUVs, specifically in high precision missions.

1.4.2. SMC control schemes

The persistent sea loads combined with high nonlinear coupling in the dynamic of the UUVs drastically limit the effectiveness of most of the control schemes implemented on these vehicles. These problems motivated a huge number of research outputs aiming to neutralize all the mentioned impacts. This leads to the dominance of robust control schemes in marine robotics since they are well-known for dealing with time-varying external disturbances and parametric uncertainties in general. Thus, a well-designed robust control algorithm should satisfy the main control goal for UUVs even if the vehicles are subjected to high parametric uncertainties (e.g. tether drag, payload changes, salinity, thrusters' performances variations, etc.). Thus, solving two of the challenging issues highlighted previously (i.e. complex nonlinear dynamics and high parametric uncertainties of UUVs). The most commonly used robust control scheme for nonlinear systems in the literature is SMC Hu et al. (2020), Garcia-Valdovinos et al. (2009). The philosophy of SMC architecture is that the control law is developed based on a particular sliding surface where the system converges and operates on the surface; this functionality makes SMC schemes suitable for nonlinear systems such as UUVs Ahmad et al. (2020). Before discussing the main robust control schemes proposed specifically for UUVs in the literature, we further subdivide these control schemes into two parts, as follows.

Non-model-based schemes: A model-free robust control scheme has been implemented on $Girona-500$ UUV for tracking tasks in Karras et al. (2014). The proposed control law guarantees fast convergence of the error dynamics to an arbitrarily small residual set around the desired trajectory and stays in this set all the time. Another model-free high order SMC has been introduced in González-García et al. (2021) to ensure fast and finite-time convergence of UUV's tracking error to the origin. Besides enhancing the robustness, the finite-time convergence of the error dynamics may help to minimize the energy consumption by the vehicle's thrusters Salgado-Jiménez et al. (2011). To deal with the effects of parametric uncertainties and unknown time-varying external disturbances in UUVs' tracking tasks, a second-order based SMC algorithm has been developed in Garcia-Valdovinos and Salgado-Jimenez (2011). In spite of the nonlinear and complex dynamics of the UUVs, a non-model-based nonsingular terminal SMC control scheme has been designed to compensate the dynamic model of the vehicles during depth tracking tasks in Wang et al. (2015). It is worth noting that the model-free control schemes attract the attention of the practitioners than model-based ones. The main reason is that obtaining an acceptable dynamic model of a real UUV is a difficult and tedious task. A switching PD-SMC scheme has been deployed on a specially designed reconfigurable UUV in Jin et al. (2018) to control its six DOFs. The desired motion of the vehicle determines its thrusters configuration (i.e. tilted w.r.t the vertical or horizontal axes). The well-known chattering problem of the SMC-based control scheme has been addressed through an output feedback high-order SMC (HOSMC) in Khalid et al. (2019). A high-order sliding manifold has been used to design the proposed HOSMC scheme instead of the classical linear sliding surface; then, the proposed controller has been validated on six-DOF dynamic model of $KAXAN$ UUV. Motivated by the same chattering phenomena, mentioned previously, in SMC in addition to modeling error in UUVs' dynamics, a continuous robust control scheme has been developed in Fischer et al. (2014a). The proposed control law, named Robust Integral of the Sign of the Error (RISE) control, does not require an infinite bandwidth of the control efforts to deal with time-varying uncertainties and external disturbances. A sequential quadratic programming SMC scheme has been designed in Wang et al. (2020b) for manoeuvring of the UUVs. The proposed controller resolves the critical issue of the actuators' saturation of the vehicles by solving a mixed minimum problem with a variable criterion in order to allocate the optimal control input to the actuators

Model-based schemes: Terminal SMC (TSMC) schemes are famous for their effectiveness in several high precision applications when compared to the traditional SMC-based techniques in terms of the fast and finite-time convergence of the tracking error dynamics to the origin. To emphasize this claim, a TSMC has been proposed to resolve the tracking problem of UUVs in Elmokadem et al. (2017). On the other hand, the proposed control law has been validated only using numerical simulations. It is obvious that the performance of a control scheme proposed for UUVs depends on the accuracy of their propulsion system (e.g. thrusters or control surfaces), which is generally driven by electric motors. Thus, the failure of the motor can definitely result in the complete system malfunctioning. Therefore, a thruster fault tolerance has been investigated extensively in different research works Hao et al. (2019). The drifting of most UUVs from the desired trajectory is mainly caused by the sea loads (e.g. ocean currents and waves). To neutralized the effects of the sea loads, an error transformation has been integrated into the sliding surface of TSMC using piece-wise function in Liu et al. (2021b). In order to alleviate the chattering phenomenon, an l_∞ norm-based minimization technique has been developed for control forces allocation of the UUV's thrusters in Soylu et al. (2007). Furthermore, a θ-D based robust control scheme has been presented in Pan and Xin (2012) for depth control of UUVs. The authors exploit the θ-D techniques to resolve the formulated optimization based tracking problem Zhou and Li (2014). We can critically notice that these proposed SMC-based control schemes often require prior knowledge of the uncertainties bounds. This is difficult to obtain in many real-time operations due to various uncertainties in the marine environments. For instance, when stray algae fix itself on the vehicles, many dynamic parameters of the vehicle's may vary instantly.

1.4.3. Adaptive control schemes

In spite of the notable performance of SMC based control algorithms, the tracking precision of such controllers is sometimes drastically affected in critical sea loads conditions. This issue is mainly caused by the static feedback parameters of most of the controllers. To resolve the tracking problem concerning SMC based control schemes, many automatic control research communities proposed another class of control algorithms that can auto-adjust their feedback gains online in different operating conditions Zhang and Wei (2017). Indeed, this concept results in another hot area of research called adaptive control. Following this philosophy, the control scheme is equipped with a special adaptive mechanism to help them in adjusting the control parameters automatically to meet various desired control objectives. Hence, addressing the challenging issues faced by UUVs in terms of the complex nonlinear dynamics as well as the high parametric uncertainties of such vehicles. It is worth noting that this research area is almost as old as the field of automatic control Annaswamy and Fradkov (2021). The control schemes are further classified into two as follows.

Non-model-based schemes: A non-regressor based adaptive control scheme has been implemented on $ODIN$ UUV in Yuh et al. (2001). This control scheme adjusts its feedback gains online in order to neutralize the effect of uncertainties and external disturbances by estimating the constant bounded parameters of the vehicle's dynamics. Taking into account the high uncertainties of UUVs' dynamics, an adaptive control scheme has been proposed to deal with the tracking problem of the vehicles in Antonelli et al. (2003). The closed-loop error dynamics, in this work, has been formulated using quaternions to avoid a possible singularity in terms of the error dynamics representation. Even though this control scheme utilizes a small part of the vehicle's dynamics, it can be considered as a non-model-based scheme. Similarly, another adaptive control scheme has been designed in Antonelli (2003). The impact of both the water currents and the time-varying disturbances has been taken into account in the proposed control structure. In line with this idea, an optimal adaptive non-model-based control scheme has been implemented on a UUV simulator in Safaei and Mahyuddin (2018). In the proposed control scheme, two different adaptive mechanisms have been developed to estimate the unknown parts of the UUV's dynamics online. Moreover, the formulated tracking problem has been solved through the minimization of a predefined objective function. Extending this control architecture to a real vehicle can explore its potential for dealing with the tracking control problems in real-life applications.

Model-based schemes: In view of all the advantages of the well-known PD+ control scheme Kelly et al. (2006), the structure of this controller has been reformulated and equipped with an adaptive mechanism to enhance its robustness in Tijjani and Chemori (2021). The improved control scheme has been validated numerically using *Leonard's* UUV simulator. To deal with the negative effects of the parametric uncertainties commonly associated with the UUVs' dynamics, an adaptive control scheme has been proposed in Sahu and Subudhi (2014). Although the adaptation law has been formulated using a regressor based technique, which utilizes the desired state, the proposed control scheme provides consistent estimations of the hydrodynamic uncertainties in different conditions. To extend the applications of the theoretical Port-Hamiltonian concept, a UUV tracking control problem has been formulated using this theory in Jia et al. (2020). From the signal processing point of view, the proposed scheme can be easily implemented on real UUVs. A region tracking task has been demonstrated using a UUV controlled with an improved Nussbaum based function adaptive controller in Liu et al. (2021c). In the proposed control scheme, the tracking error dynamics has been reformulated with the help of the barrier Lyapunov functions. The notable advantage of this control scheme, when compared to the convention prescribed control schemes, lies in its capacity to smooth the control input signals. Also, an enhanced Nussbaum function (see Chen (2019)) has been developed to derive the error dynamics into the region of interest without exceeding the vehicle's actuators dead zone. This idea has been further confirmed using Lyapunov stability tools. Furthermore, an adaptive nonlinear state feedback control scheme has been deployed on a UUV named *AC-ROV* in Maalouf et al. (2015b). In a similar way, an $\mathscr{L}_1$ adaptive control scheme has been developed and implemented on the same *AC-ROV* in Maalouf et al. (2015a). The decoupling characteristic of the proposed control scheme results in smooth and stable adaptive behavior of the vehicle. Also, the obtained experimental results have shown the effectiveness of the proposed control scheme towards time-varying parametric uncertainties as well as external disturbances rejection. To deal with the issue of tracking time lags of the $\mathscr{L}_1$ adaptive control law, due to the presence of an embedded filter in this controller, an extended version of the control architecture has been proposed in Maalouf et al. (2013).

In spite of the auto-adjustment mechanism provided by adaptive control schemes, online estimation of the UUV's uncertain dynamics (e.g. hydrodynamics) can be computationally intensive Antonelli et al. (2003). Besides parametric sensitivity issues, designing the adaptation gains for these schemes is a tedious task. From the practical point of view, many states of the UUVs are inaccessible. In view of all these issues, a possible solution can be implementing an observation-based control scheme on these vehicles to deal with their tracking control problems. Hence, this class of control schemes is revisited subsequently.

1.4.4. Observation-based control schemes

We can critically observe that most of the authors proposed their control schemes based on the strong assumption that the full-states measurements are always available. The full-state measurements are inaccessible in practice for the case of many systems including UUVs, as discussed previously Baruch et al. (2020). This issue has motivated a lot of research output concerning observers; the main reason is that the observers can resolve the problems of inaccessible states, as well as the expensive cost of sensors of the UUVs pointed out in section 1.3. Thus, different observer design techniques have been proposed in the literature for UUVs, as follows.

Non-model-based schemes: A model-free adaptive control scheme (MFAC) has been proposed in Li et al. (2020) as a completely model-independent scheme for UUVs tracking control. Moreover, a data-driven extended state observer has been introduced into the MFAC structure to estimate the vehicle's dynamics in real-time using an approximation error generated in the pseudo-Jacobian matrix. Also, a nonlinear disturbance observer (NDOB) has been coupled with conventional PD to control a hovering UUV in Bi and Feng (2019). Furthermore, a model-free observer has been proposed in Izadbakhsh et al. (2019). The proposed controller/observer scheme has been developed using function approximation techniques combined with StoneâĂŞWeierstrass theorem of a differential equation. The main advantage of the proposed scheme lies in its simplicity and reducing complexity in terms of the dimensions of regressor matrices. This scheme can be extended to the case of UUVs since their dynamics is difficult to obtain. Another critical issue is the need for velocity error in the design of most of the control schemes proposed for UUVs. It is well-known that the velocity measuring sensor for UUV is too expensive for low-cost UUVs. For this reason, a fuzzy observation-based tracking control scheme has been investigated in Duan et al. (2020). The proposed observer in this scheme has a simple linear structure which contradicts many observer designs proposed for UUVs from the literature. Observers are also often used to control a fleet of UUVs. For instance, a line-of-sight (LOS) formation control scheme based on a constrained angle, for multi-agent UUVs, has been investigated in Gao and Guo (2019). To deal with the communication issues between the agents, an observer has been designed for estimating the leader's velocity as accurate as possible in a finite time. Additionally, an ln-type barrier Lyapunov function has been exploited to demonstrate the uniformly ultimately bound property of the error dynamics.

Model-based schemes: An observation-based finite-time output feedback control scheme has been developed to deal with the tracking problem of UUV in Li et al. (2015). To avoid the issue of a possible singularity in the attitude of the vehicle, a quaternions representation has been adopted. The authors coupled a finite-time observer to their proposed stabilizing controller for velocity estimation. LasalleâĂŹs invariance principle has been used to study the stability of the closed-loop dynamics. Disturbance observation is another key strategy used to improve a control scheme in addition to the full-state estimation. To demonstrate the effectiveness of this technique in real-time marine applications, an extended state observer (ESO) has been proposed for two DOFs trajectory tracking of UUV in Guerrero et al. (2020b). In line with this idea, an external disturbance observer (EDO) has been added to backstepping and NPD+ based controllers to improve the UUV's tracking performance in Guerrero et al. (2020a). One of the main aspects of these two papers is that the proposed controller/observer schemes have been validated in real-time experiments. However, the main problem of the proposed controller/observer schemes lies in their requirement of an expert knowledge transfer. Similarly, a disturbance observer-based control has been proposed in Su et al. (2016) to resolve the technical problem in switched stochastic systems. This control scheme has been extended to cover the class of systems like UUVs in Cui et al. (2017). Contrary to the majority of the proposed control schemes for UUVs, the proposed control scheme has been validated through real-time experiments. To compensate for the negative effect of actuators' dead-zone nonlinearity, which deteriorates the tracking precision of UUVs, an NDOB has been introduced into the structure of the SMC controller in Cui et al. (2016). Based on the theoretical development in the work of Wang et al. (2020a), the proposed predictive-based observer can be extended and deployed on UUVs to deal with the problem of the delays, especially in low-cost multi-agent vehicles for intervention operations.

1.4.5. MPC control schemes

Even though a vast number of advanced control methods have been proposed for UUVs, most of them do not consider missions constraints. For this reason, MPC and MPC-based control schemes are proposed to effectively deal with the issue of these constraints while satisfying the optimal control objectives Shi and Zhang (2021). Another advantage of these schemes is they are often used for cooperative underwater missions involving homogeneous or heterogeneous multi-agent UUVs. Hence, these control schemes address many control problems for UUVs, as pointed out previously in challenging issues, like model inaccuracies, time-varying disturbances, parametric uncertainties, collision avoidance, etc. Based on these qualities, a number of MPC-based control schemes have been proposed in the literature as follows. To deal with the problems of tracking and formation control of the low-cost multi-agents UUVs, a receding horizon-based formation and tracking control algorithm has been designed in Li et al. (2017). The authors propose to formulate an objective function for each UUV (agent) through a detailed analytical design in the proposed control architecture. However, the potential of the proposed control scheme for real-life applications has not been investigated. The bandwidth limitation of the mechanical actuators in the propulsion systems of low-cost UUVs becomes a constraint to most of the control schemes proposed for such vehicles; any attempt to operate the actuators outside this constraint can result in an unstable closed-loop marine behavior. Although MPC-based control schemes are well-known in dealing with the issues of constraints, these schemes are not so excellent in rejecting stochastic time-varying disturbance. For this reason, an antidisturbance constrained control scheme has been proposed in Peng et al. (2019) to address the problems of parametric uncertainties and constraints for UUVs through exploiting the advantages of the command governor (COG). To enhance the efficiency of the MPC for trajectory tracking tasks of small-sized UUVs, a super twisting algorithm (STA) has been integrated into the structure of the control scheme in Wang et al. (2018a). The issue of a speed jump due to a high initial tracking error has been addressed in Gan et al. (2018). In this work, the authors propose to design a quantum-behaved particle swarm optimization algorithm to compute the desired velocity signals for the dynamic controller. This idea limits the velocity signals to a specific desired range. A Lyapunov-based MPC scheme has been developed in Shen et al. (2018) to improve the efficiency of the tracking control performance for the UUVs. The main advantage of the proposed controller lies in its online lightweight computational framework. Even though some sufficient stability conditions have been established to ensure the recursive feasibility of the formulated objective function of this scheme, only numerical simulations have been used to prove the stable behavior of the scheme. Furthermore, a radial basis function has been equipped with the Levenberg-Marquardt-Error compensation technique to improve the tracking performance of NMPC in Chu et al. (2021). Another advantage of this control scheme worth to be mentioned is its ability to estimate the vehicle's model offline. Although a tracking error improvement of 25 % has been obtained when compared to the conventional MPC scheme, this result has only been achieved through numerical simulations.

1.4.6. Combined control schemes

Although the literature on UUVs' tracking control schemes has reached a certain level in terms of maturity, it is well-known that most of these proposed control algorithms are applications specific. Hence, it is impossible to find a single control algorithm with an excellent closed-loop stability behavior to suit many real-life marine operations. For this reason, the conventional practice in various marine applications is to hybridize two or more control strategies to satisfy different control objectives, thereby resolving most of the challenging issues mentioned previously. Based on this notion, the strengths of a specific control approach are preserved while complementing its drawbacks by carefully exploiting the advantages of another control structure. For instance, the robustness of an SMC-based scheme is degraded by its static feedback gains in several marine applications; therefore, equipping this control scheme with a computationally light adaptive mechanism to auto-adjust the controller gains online will definitely result in a better performance. The main combined control (non-model-based and model-based) schemes proposed for the UUVs tracking control, selected from the literature, include the following.

Non-model-based schemes: It is commonly known that the hydrodynamic coefficients, internal perturbations, and time-varying external disturbances are generally difficult to measure or estimate with a certain accuracy; therefore, this issue leads to the inefficiency of the majority of the model-dependant controllers. For this reason, a model-free control scheme, subject to the uncertainties as well as actuators saturation, has been proposed in Yu et al. (2020) for the seafloor exploration task using a UUV. Besides taking into account the dynamics of the actuator in the proposed control structure, an extra compensator has been integrated to deal with any undesired control signals truncation due to saturations. Barbalat lemma has been used to study the stability behavior of the resulting closed-loop dynamics. The authors validated the proposed control law through numerical simulations. A neural network (NN) based robust control scheme has been proposed in Eski and Yildirim (2014) to resolve the tracking problem of UUVs. The proposed control law has been developed by combining two different algorithms (i.e. an SMC and NN based control schemes). It is obvious that any control scheme depending mainly on the exact dynamic model of a system can be challenging to deploy on UUVs in practice. Thus, a second-order SMC (2nd-OSMC) scheme has been demonstrated in the literature as one of the most effective control schemes for dealing with the impacts of time-varying parametric uncertainties and stochastic external disturbances. From the practical perspective, the performance of this control scheme is often far from the desired control objectives, especially in high precision marine tasks. To resolve this problem in 2nd-OSMC, an auto-tuning algorithm based on backpropagation NN has been introduced to the control scheme in García-Valdovinos et al. (2019). The proposed control scheme has been implemented on a mini-remotely operated UUV for experimental validation. Similarly, a learning-based adaptive control scheme has been proposed in Qiu et al. (2021), where a radial basis function NN has been designed to approximate the unknown dynamics of the UUVs subject to unknown uncertainties. To resolve the high computational cost of the NN, a command filter has been added to the structure of the proposed control scheme. Even though the stability analysis of the resulting closed-loop dynamics has been successfully conducted, the potential of this scheme has been only shown through numerical simulations. It is worth noticing that actuator saturation occurs often even when model-free controllers are used for UUVs Jiang et al. (2021). This critical issue is noticed often for long-duration missions. Therefore, actuator failure has been investigated in the literature. To address this problem of the actuator failure, a model-free control scheme has been proposed in Zhu et al. (2021) for tracking control of UUVs subject to the time-varying external disturbances. Similar to many control schemes proposed in the literature, the effectiveness of this control approach has been validated only through theoretical studies and numerical simulations.

Model-based schemes: One of the persistent issues in an advanced feedback control scheme is the performance degradation caused by the problem of quantization. This effect may often result in an unstable behavior of a resulting closed-loop dynamics in many real systems, typically for the case of physical systems with different kinds of sensors and actuators like UUVs. Despite this problem, only a few number of research works are available from the literature concerning this aspect. Some of the tracking control schemes proposed to resolve the effects of quantization in control inputs include the control law developed in recently in Yan and Yu (2018). In this control scheme, an SMC architecture has been developed where the quantization error bound is embedded in the switching/robust function of the controller. The need for high precision tracking and fast dynamic response in various underwater intervention operations lead to the design of an adaptive-based TSMC in Wang et al. (2016). Compared to the conventional TSMC from the literature, the proposed controller does not require prior knowledge of the bound of the lumped uncertainties. The effectiveness of this scheme has not been validated for any real-time application. Similarly, an adaptive second-order fast nonsingular TSMC scheme (ASFNTSMC) has been designed for tracking control of UUVs subjected to parametric uncertainties, internal perturbations, and time-varying external disturbances in Qiao and Zhang (2019). The main advantage of this scheme is once the tracking error hits the proposed sliding surface, the control scheme ensures that the error slides on the surface to the origin and remain there all the time. Numerical simulations have been used to investigate the efficiency of the proposed scheme in two different scenarios. In Xu et al. (2015), the authors proposed to combine the advantages of SMC and backstepping controllers in order to counteract the uncertainties and persistent external disturbances affecting UUVs during missions. Additionally, an adaptation law has been designed, and a virtual dynamics has been formulated to function as velocity errors to define the UUV's attitude errors. The potential of the NN to approximate nonlinear functions through learning their behavior has been exploited to enhance the performance of various controllers in the automatic control community. It is worth noting that this functionality of the NN can be exploited for the case of the highly nonlinear dynamics of the UUVs for control law design. Following this philosophy, an adaptive NN control scheme has been proposed to resolve the trajectory tracking problem of UUVs in Miao et al. (2013). The authors have also shown the resulting closed-loop dynamics is uniformly ultimately bounded (UUB). On the other hand, the main drawback of most of the NN based control schemes is a high computational cost caused by the learning time, which multiply with the weights of hidden layers. Also, an intelligent adaptive controller combining NN and fuzzy logic has been proposed for UUVs in Hassanein et al. (2016). Online identification and adaptive algorithms of the proposed control schemes use the concept of semi-serial-parallel-model to compute the desired control input signals. Recently, a hybrid control scheme has been proposed for a UUV taking into account the influences of structured/unstructured uncertainties in Kumar and Rani (2020). To counteract the effects of the external disturbances as well as the NN reconstruction error, both a compensator and a radial basis function have been integrated into the proposed control structure. The robustness of the controller has been demonstrated based on numerical simulations. Despite the effectiveness of the combined control schemes, several marine operation may require a high precision tracking controller for a single or multi-agent UUVs in order to satisfy a specific control objective.

Remark 2. *It is worth noting that this class characterizes those methodologies combining two or more techniques in their design. For instance the adaptive-based TSMC, proposed in Qiao and Zhang (2019), Wang et al. (2016), combines "Adaptive control" and "Sliding mode control" techniques; consequently, it can be either classified in the class of "Adaptive control schemes" or in the class of "SMC control schemes". However, sometimes it is difficult to decide which class and where we can place these kinds of control schemes mentioned above. To avoid such an ambiguity in the categorization of these control schemes, we created this class we named "combined control schemes". It is not a trivial task to include them in Table 1 since the domain of these control schemes is too broad. This implies that the designer has a total control over selecting the main fundamental control laws to satisfy the desired control objectives. Accordingly, we removed this class from Table 1.*

1.4.7. Multi-UUV cooperation control issue

In many applications, a solo operation of a robot is not always sufficient to deal with several problems during intervention operations. Hence, the cooperation of multiple robots is necessary for such missions. For this reason, the cooperation of multiple robots, such as UUVs, is becoming a hot research topic in robotics and automatic control research communities. Therefore, the design of multi-UUV control schemes (e.g. cooperative formation control, cooperative navigation, and cooperative confrontation of the multi-UUV) has gained significant attention in recent years from the communities mentioned above Liu et al. (2020).

Remark 3. *Note that this survey focuses more on tracking control of a single UUV. Since we only have a single UUV at our disposal and a laboratory-scale testing pool for the real-time validation of all the representative control schemes in this paper.*

Based on *remark 3*, we briefly review some representative results on multi-UUV cooperative control as follows. A heuristic fleet cooperation algorithm, based on an evolutionary approach to solve multi-vehicle dynamic task assignments, has been proposed in Abbasi et al. (2022). The proposed scheme has been validated on multiple UUVs for a marine mission to control the problem of Crown-Of-Thorns Starfish (COTS) in QueenslandâĂŹs Great Barrier Reef. To deal with the issues of acoustic ranging error in underwater cooperative localization, when multiple leader UUVs play the role of communication and navigation aids (CNA), an adaptive cubature Kalman filter (ACKF) has been proposed in Xu et al. (2021). For multiple UUVs to move accurately and continuously towards the desired target approaching in anchor-free underwater environments, a scalable cooperative localization has been proposed in Li et al. (2022). The main advantage of the proposed scheme is that many constraints, such as the kinematic and communication limitations, collision, and obstacle avoidance of multiple vehicles have been considered at the development stage of the algorithm. Similarly, a cooperative path planning scheme for heterogeneous vehicles consisting of UUVs, unmanned aerial vehicles (UAVs) and unmanned surface vehicle (USVs) has been developed in Wu et al. (2020). To meet the high demand for low latency and low power consumption in a collaborative data collection using a fleet of UUVs, a composite algorithm of multi-UUV task allocation and Q-learning-based UUV path planning has been proposed in Han et al. (2021). This technique simplifies the complex methods for marine data collection tasks for the case where a single UUV is deployed for such difficult missions. It is worth noting that disturbances are difficult to measure, and their bounds are often unknown in many marine applications. Furthermore, the nonlinearities and delays of different sensors installed on marine robots complicate the control system design for such systems de CossÃŋo et al. (2020). A cascade structure-based predictive observer, proposed recently in Wang et al. (2020a), can be deployed on UUVs to deal with the problem of the delays, especially in multi-agent vehicles for intervention operations. Taking into account this delay issue, a tracking control problem has been addressed in Yan et al. (2020a) for single vehicle and multi-agent cases. However, in the real-time experiments conducted by these researchers, critical scenarios, such as robustness and external disturbances tests, have not been considered. For more details on multi-UUV cooperative control, the reader can refer to Zhang et al. (2022), Wang et al. (2022), Sun et al. (2022), Wu et al. (2021), Shi et al. (2021), etc.

A summary of the strengths and weaknesses of the main control solutions, as discussed above, implemented on the UUVs using some selected criteria is given subsequently.

1.5. Strengths and weaknesses of the existing solutions

The main existing control schemes, proposed and implemented for UUVs either through numerical simulation or by experiments in the last two decades, have been reexamined in this survey. A simple but clear classification has been proposed w.r.t some key features common to all the classes of the control schemes discussed previously. Although the proposed classification is not exhaustive due to the maturity level of the literature concerning automatic control/robotics, a critical comparative study of these schemes can definitely help to point out the strengths and weaknesses of each respective class. This approach can provide an overview as well as background information for early career researchers and practitioners to propose new control schemes, with potential in many real-time marine applications, to resolve the tracking control issues of UUVs. Based on Fig. 1, Table 1 summarizes the strengths and weaknesses of each class of the proposed control schemes from the literature.

Table 1
Summary of the Strengths and Weaknesses of Different Classes of Control Schemes Proposed for UUVs.

Summary of criteria-based comparative study							
Main control schemes	**Selected criteria**						
	Implementation simplicity	*Robustness to uncertainties*	*Disturbances rejection*	*Sensitivity to sensor noise*	*Tuning simplicity*	*Computational time*	*Tracking precision*
PD/PID based	+++++	+	+	+++	+	+++++	++
SMC based	+++	++++	+++	+++	+++	+++	+++
Adaptive based	+++	+++	+++	++++	+++	++	+++
Observation based	+	++++	+++	+++	+	+	+++
MPC based	+	+++	+++	++	+	+	+++

Note: *excellent = +++++, good = ++++, average = +++, poor = ++, and bad = +. This table clearly shows that the combined control schemes can have high precision tracking functionality when carefully designed.*

1.6. Survey Contributions and Organization

The main contributions of the present review are detailed as follows:

1. This paper presents and discusses a review of the key efforts made for the last two decades. A special attention is given to the tracking control of a complex robotic system such as UUV. Compared to the survey papers on control from the literature (e.g. Gan et al. (2017), Xiang et al. (2018), Karimi and Lu (2021), Neira et al. (2021), Kumar and Mondal (2021), Gambhire et al. (2021), Liu et al. (2022), etc.), this paper focuses more on bridging the wide gap, always existing, between theoretical design and the real-time implementation of fundamental tracking control schemes, especially for the case of UUVs tracking control problem. Even though a few recent survey papers like Bhattacharyya (2017), Morato et al. (2020), Kamel et al. (2020), Theunissen et al. (2021), and Shi and Zhang (2021) present some results from several research papers, almost all the review papers available in the literature fail to report any results validated through real-time experiments. Indeed, most of these surveys do not cover a class of special uncertain coupled multiple-input multiple-out (MIMO) nonlinear systems representing UUVs.
2. Another contribution of this paper, worth to be mentioned, lies in the consolidation of all the aspect of typical control system design for complex robotic systems, that is, from modeling to controller design as well as real-time implementation. In fact, this approach is also missing in many of the survey papers available in the literature. For this reason, the design techniques of some representative tracking control schemes from the proposed classes of the control schemes, investigated herein, are provided. This will serve as a key example of how to design a control scheme, as well as how to implement it on a real UUV, for early career researchers and practitioners in the field of automatic control. Additionally, this paper can be considered as a tutorial for readers from other sub-domains, like marine robotics, which are closely related.
3. Rigorous scenario-based real-time experiments are conducted using *Leonard UUV* for a critical study of the proposed representative control schemes. Although some good simulation results of the proposed representative tracking control schemes for UUVs are reported in the literature, we faced several challenges, including (i) a bad tracking in real-life applications, (ii) the impossibility to extend some of them to the case of real UUVs Martin and Whitcomb (2018), etc.
4. Furthermore, available investigation gaps are discussed to open and guide the possible future research directions, which will certainly further enrich the literature on UUVs tracking control.

The rest of this paper is structured as follows. Section 2 describes the modeling process of UUVs. The design of the proposed representative control schemes, some technical aspects of the vehicle, *Leonard UUV* used for experimental validations, as well as the proposed real-time scenarios in this paper, are discussed in Section 3. Furthermore, the obtained experimental results of the proposed representative

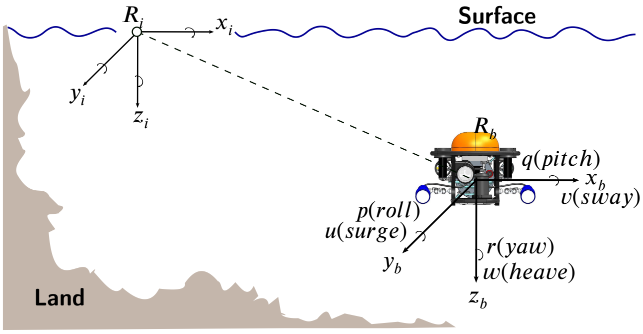

Figure 2: Illustration of the inertial reference frame (R_i) and body-fixed reference frame (R_b) fixed to *Leonard UUV* for its kinematic and dynamic modeling.

tracking control schemes, and their comparative studies, are presented in the same section. Some potential investigation gaps and future trends are introduced in Section 4, while Section 5 finalizes this survey paper with concluding remarks.

Remark 4. *Note that this survey paper gives an overview of tracking control schemes for UUVs. It is not our aim to detail a complete bibliography. Therefore, we propose to contribute by a subjective review of the recently proposed tracking control schemes applied to UUVs. Also, it is worth mentioning that experimental validations of tracking control schemes for UUVs based on realistic scenarios have been one of the complex issues in UUVs technology in the first decade of the 21st century Ridao et al. (2015).*

2. Modeling of Underwater Vehicles

The main goal of this survey is to study the tracking control issues concerning UUVs. In general, designing high precision control schemes often, especially model-based ones, require an approximate knowledge of the system dynamics to be controlled. In view of this reason, we propose to improve slightly the conventional theoretical representation of UUVs. Therefore, the position and orientation of the UUVs in six DOFs can be determined using two unique reference frames, each based on a six coordinates system, as illustrated in Fig. 2. These reference frames are generally named based on the standard set by SNAME (Society of Naval Architects and Marine Engineers), as in the following Fossen (2002) Maalouf et al. (2015a):

1. The inertial reference frame R_i. The R_i frame is located mostly at the surface of the water body.
2. The body-fixed reference frame R_b. This frame usually corresponds to the vehicle's center of volume.

Note that it is convenient to define the linear motions of UUV about its R_b frame as *surge*, *sway*, and *depth* (illustrated in Fig. 2). Similarly, the corresponding rotational motions of the vehicle can be described as *roll*, *pitch*, and *yaw*.

In most cases, the modeling of UUVs is categorized into kinematics and dynamics, which are detailed as follows.

2.1. UUV's Kinematics

Based on Fig. 2, the kinematics of UUV relating the first time-derivatives of the vehicle's position and attitude in R_i frame with their corresponding linear and angular velocities, expressed in R_b frame, is formulated in vector form as follows:

$$\dot{\boldsymbol{\eta}} = \boldsymbol{J}(\boldsymbol{\eta})\boldsymbol{\nu} \tag{1}$$

where $\boldsymbol{\nu} = [\boldsymbol{\nu}_1 \ \boldsymbol{\nu}_2]^T$ is the vector of linear and angular velocities of the vehicle in R_b frame, $\boldsymbol{\nu}_1 = [u \ v \ w] \in \mathbb{R}^{3\times1}$ and $\boldsymbol{\nu}_2 = [p \ q \ r] \in \mathbb{R}^{3\times1}$, $\boldsymbol{\eta} = [\boldsymbol{\eta}_1 \ \boldsymbol{\eta}_2]^T$ defines the vector of position and attitude express in R_i frame, $\boldsymbol{\eta}_1 = [x \ y \ z] \in \mathbb{R}^{3\times1}$ and $\boldsymbol{\eta}_2 = [\phi \ \theta \ \psi] \in \mathbb{R}^{3\times1}$, while $\boldsymbol{J}(\boldsymbol{\eta}) \in \mathbb{R}^{6\times6}$ is a matrix defining the 3D spacial transformation between R_i and R_b frames.
This so-called transformation matrix $\boldsymbol{J}(\boldsymbol{\eta})$, in the kinematic formulation (1), is expressed as Fossen (1999):

$$\boldsymbol{J}(\boldsymbol{\eta}) = \begin{bmatrix} \boldsymbol{J}_1(\boldsymbol{\eta}_2) & \mathbf{0}_{3\times3} \\ \mathbf{0}_{3\times3} & \boldsymbol{J}_2(\boldsymbol{\eta}_2) \end{bmatrix} \tag{2}$$

with $\boldsymbol{J}_1(\boldsymbol{\eta}_2)$ and $\boldsymbol{J}_2(\boldsymbol{\eta}_2)$ given by (3) and (4) respectively, as:

$$\boldsymbol{J}_1(\boldsymbol{\eta}_2) = \begin{bmatrix} c\psi c\theta & c\psi s\theta s\phi - s\psi c\phi & c\psi s\theta c\phi + s\psi s\phi \\ s\psi c\theta & s\psi s\theta s\phi + c\psi c\phi & s\psi s\theta c\phi - c\psi s\phi \\ -s\theta & c\theta s\phi & c\theta c\phi \end{bmatrix} \tag{3}$$

$$\boldsymbol{J}_2(\boldsymbol{\eta}_2) = \begin{bmatrix} 1 & s\psi t\theta & c\psi t\theta \\ 0 & c\psi & -s\psi \\ 0 & s\phi/c\theta & c\phi/c\theta \end{bmatrix} \tag{4}$$

where $cx^\star$, $sx^\star$, and $tx^\star$ denoting $cosx^\star$, $sinx^\star$, and $tanx^\star$ functions respectively, with $x^\star \in \{\phi, \theta, \psi\}$.

Remark 5. *The UUV kinematic formulation (1) may be undefined and non-invertible when the vehicle's pitch angle $|\theta| \to \frac{\pi}{2}$ due to a possible singularity in $\boldsymbol{J}_2(\boldsymbol{\eta}_2)$. The main cause of this singularity is the representation of UUV's attitude using Euler angles. This issue can be addressed using quaternions to describe the attitude of the UUV for a marine task where the vehicle may be operated at $|\theta|_{max} \approx \frac{\pi}{2}$ Ali et al. (2020), Borlaug et al. (2021). However, a representation based on quaternions requires normalization of all its four parameters such that the square of their norm is unity. A slight measurement noise from the vehicle's sensor or computational round-off could destabilize this normalization.*

Taking *remark 5* into account, in this survey, we carefully design the desired pitch angle θ_d such that it is sufficiently far away from the neighbourhood of $\theta = \pm\frac{\pi}{2}$. Therefore, $\boldsymbol{J}_2(\boldsymbol{\eta}_2)$ and $[\boldsymbol{J}_2(\boldsymbol{\eta}_2)]^{-1}$ are invertible and well defined in our case.

2.2. UUV's Dynamics

The dynamics describing the six DOFs motions of UUVs, based on the mathematical formulations proposed in Fossen (2002), Fossen (1999) and inspired by the representation in Antonelli et al. (2008) as well as using SNAME standard notations, can be expressed in the vehicle's R_b frame as follows:

$$\boldsymbol{M}\dot{\boldsymbol{\nu}} + \boldsymbol{C}(\boldsymbol{\nu})\boldsymbol{\nu} + \boldsymbol{D}(\boldsymbol{\nu})\boldsymbol{\nu} + \boldsymbol{g}(\boldsymbol{\eta}) = \boldsymbol{\tau} + \boldsymbol{w}(t) \tag{5}$$

where $\boldsymbol{M} \in \mathbb{R}^{6\times6}$ is the vehicle's inertia matrix, including the effect of the added mass, $\boldsymbol{C}(\boldsymbol{\nu}) \in \mathbb{R}^{6\times6}$ is the Coriolis and centripetal matrix, with added mass effect included, $\boldsymbol{D}(\boldsymbol{\nu}) \in \mathbb{R}^{6\times6}$ is the damping matrix, $\boldsymbol{g}(\boldsymbol{\eta}) \in \mathbb{R}^{6\times1}$ is the vector of the gravitational and the buoyancy forces as well as the restoring moments, $\boldsymbol{\tau} \in \mathbb{R}^{6\times1}$ is the vector of the control inputs generated by the vehicle's thrusters, and $\boldsymbol{w}(t) \in \mathbb{R}^{6\times1}$ is a time-varying vector of internal/external disturbances (e.g. sensor measurements noise, currents, and waves).
Furthermore, the following assumption is considered in (5).

Assumption 1. *The UUV body is assumed to be rigid, and the R_i frame is well fixed. Hence, the forces between the vehicle's components as well as the forces caused by the rotation of the Earth are considered to be negligible.*

It is worth noting that, in a real-time marine application, the dynamics of UUVs (e.g. *Leonard UUV*) in (5) is highly nonlinear and unknown. This complex behavior results due to the nature of the matrices and vectors of the dynamics (5). For instance, the matrices $\boldsymbol{M}$ and $\boldsymbol{C}(\boldsymbol{\nu})$ of dynamics (5) are partly known, $\boldsymbol{D}(\boldsymbol{\nu})$ is highly uncertain due to the unmodeled hydrodynamic effects, and $\boldsymbol{g}(\boldsymbol{\eta})$ can be approximately computed but may contain some computational uncertainties. Thus, taking into account the uncertainties mentioned above in the model of the vehicle may improve its dynamics (in (5)). Although various research works in literature proposed to modify slightly the dynamics of UUV to capture all the uncertainties, see for instance Ali et al. (2020), most of these works only consider some of these uncertainties in their dynamic model representations. Hence, we propose to include all the uncertainties into (5) as follows:

$$\boldsymbol{M}^\star\dot{\boldsymbol{\nu}} + \boldsymbol{C}^\star(\boldsymbol{\nu})\boldsymbol{\nu} + \boldsymbol{D}^\star(\boldsymbol{\nu})\boldsymbol{\nu} + \boldsymbol{g}^\star(\boldsymbol{\eta}) = \boldsymbol{\tau} + \boldsymbol{w}^\star(t) \tag{6}$$

where $\boldsymbol{M} = \boldsymbol{M}^\star + \Delta\boldsymbol{M}^\star$, $\boldsymbol{C}(\boldsymbol{\nu}) = \boldsymbol{C}^\star(\boldsymbol{\nu}) + \Delta\boldsymbol{C}^\star(\boldsymbol{\nu})$, $\boldsymbol{D}(\boldsymbol{\nu}) = \boldsymbol{D}^\star(\boldsymbol{\nu}) + \Delta\boldsymbol{D}^\star(\boldsymbol{\nu})$, and $\boldsymbol{g}(\boldsymbol{\eta}) = \boldsymbol{g}^\star(\boldsymbol{\eta}) + \Delta\boldsymbol{g}^\star(\boldsymbol{\eta})$.
This improved representation of the dynamic matrices and vectors can be generalized as follows:

$$\boldsymbol{X}(\cdot) = \boldsymbol{X}^\star(\cdot) + \Delta\boldsymbol{X}^\star(\cdot) \tag{7}$$

where $\boldsymbol{X}^\star(\cdot)$ defines the nominal part (i.e. the true value) and $\Delta\boldsymbol{X}^\star(\cdot)$ denotes the uncertain part (i.e. unknown part).
Consequently, the time-varying disturbance vector $\boldsymbol{w}(t)$ is combined with the uncertainties and rewritten as follows:

$$\boldsymbol{w}^\star(t) = -\Delta\boldsymbol{M}^\star\dot{\boldsymbol{\nu}} - \Delta\boldsymbol{C}^\star(\boldsymbol{\nu})\boldsymbol{\nu} - \Delta\boldsymbol{D}^\star(\boldsymbol{\nu})\boldsymbol{\nu} - \Delta\boldsymbol{g}^\star(\eta) + \boldsymbol{w}(t) \tag{8}$$

To simplify control algorithm design for UUVs as well as the overall closed-loop stability analysis, the dynamics (6) can be transformed and expressed in R_i frame as follows:

$$\boldsymbol{M}^\star_{\boldsymbol{\eta}}(\boldsymbol{\eta})\ddot{\boldsymbol{\eta}} + \boldsymbol{C}^\star_{\boldsymbol{\eta}}(\boldsymbol{\nu},\boldsymbol{\eta})\dot{\boldsymbol{\eta}} + \boldsymbol{D}^\star_{\boldsymbol{\eta}}(\boldsymbol{\nu},\boldsymbol{\eta})\dot{\boldsymbol{\eta}} + \boldsymbol{g}^\star_{\boldsymbol{\eta}}(\boldsymbol{\eta}) = \boldsymbol{\tau}^\star_{\boldsymbol{\eta}}(\boldsymbol{\eta}) + \boldsymbol{w}^\star_{\boldsymbol{\eta}}(t) \tag{9}$$

where

$$\begin{cases} \ddot{\boldsymbol{\eta}} = \boldsymbol{J}(\boldsymbol{\eta})\dot{\boldsymbol{\nu}} + \dot{\boldsymbol{J}}(\boldsymbol{\eta})\boldsymbol{\nu},\ \boldsymbol{M}^\star_{\boldsymbol{\eta}}(\boldsymbol{\eta}) = \boldsymbol{J}^{-T}(\boldsymbol{\eta})\boldsymbol{M}^\star\boldsymbol{J}^{-1}(\boldsymbol{\eta}), \\ \boldsymbol{C}^\star_{\boldsymbol{\eta}}(\boldsymbol{\nu},\boldsymbol{\eta}) = \boldsymbol{J}^{-T}(\boldsymbol{\eta})[\boldsymbol{C}^\star(\boldsymbol{\nu}) - \boldsymbol{M}^\star\boldsymbol{J}^{-1}(\boldsymbol{\eta})\dot{\boldsymbol{J}}(\boldsymbol{\eta})]\boldsymbol{J}^{-1}(\boldsymbol{\eta}), \\ \boldsymbol{D}^\star_{\boldsymbol{\eta}}(\boldsymbol{\nu},\boldsymbol{\eta}) = \boldsymbol{J}^{-T}(\boldsymbol{\eta})\boldsymbol{D}^\star(\boldsymbol{\nu})\boldsymbol{J}^{-1}(\boldsymbol{\eta}), \boldsymbol{g}^\star_{\boldsymbol{\eta}}(\boldsymbol{\eta}) = \boldsymbol{J}^{-T}(\boldsymbol{\eta})\boldsymbol{g}^\star(\boldsymbol{\eta}), \\ \boldsymbol{\tau}^\star_{\boldsymbol{\eta}}(\boldsymbol{\eta}) = \boldsymbol{J}^{-T}(\boldsymbol{\eta})\boldsymbol{\tau}^\star,\ \text{and } \boldsymbol{w}^\star_{\boldsymbol{\eta}}(t) = \boldsymbol{J}^{-T}(\boldsymbol{\eta})\boldsymbol{w}^\star(t). \end{cases}$$

2.3. Properties and Features of the Dynamic Model Terms

Exploiting the dynamic terms in (6), the performance of the control schemes for UUVs can be improved by compensating the vehicle's dynamics in the control architecture. Because of this fact, it is necessary to study the properties of these terms in detail, as follows.

Property 1. *The vehicle's inertia matrix $\boldsymbol{M}^\star_{\boldsymbol{\eta}}(\boldsymbol{\eta})$ is symmetric and positive definite. Moreover, this matrix satisfies Tijjani et al. (2021):*

$$\kappa\|\boldsymbol{\eta}\|^2 \le \boldsymbol{\eta}^T\boldsymbol{M}^\star_{\boldsymbol{\eta}}(\boldsymbol{\eta})\boldsymbol{\eta} = \boldsymbol{\eta}^T\boldsymbol{M}^\star_{\boldsymbol{\eta}}(\boldsymbol{\eta})^T\boldsymbol{\eta} \le \kappa(\boldsymbol{\eta})\|\boldsymbol{\eta}\|^2 \tag{10}$$

where $\kappa \in \mathbb{R}_{>0}$ is a positive constant, $\kappa(\boldsymbol{\eta}) \in \mathbb{R}_{>0}$ is a non-decreasing positive function and $\boldsymbol{\eta} \in \mathbb{R}^{6\times1}$ is the vehicle's actual trajectory.

Property 2. *The Coriolis and centripetal matrix $\boldsymbol{C}^\star_{\boldsymbol{\eta}}(\boldsymbol{\nu},\boldsymbol{\eta})$ of a UUV in motion can be parameterized in general as a skew-symmetric matrix Fossen (2002), i.e.*

$$\boldsymbol{C}^\star_{\boldsymbol{\eta}}(\boldsymbol{\nu},\boldsymbol{\eta}) = -\boldsymbol{C}^\star_{\boldsymbol{\eta}}(\boldsymbol{\nu},\boldsymbol{\eta})^T,\ \forall\,\boldsymbol{\nu},\,\boldsymbol{\eta} \in \mathbb{R}^{6\times1} \tag{11}$$

Property 3. *The $\boldsymbol{D}^\star_{\boldsymbol{\eta}}(\boldsymbol{\nu},\boldsymbol{\eta})$ matrix of UUVs is strictly positive Fossen (2002). Hence, the matrix fulfils the following argument:*

$$\boldsymbol{\eta}^T\boldsymbol{D}^\star_{\boldsymbol{\eta}}(\boldsymbol{\nu},\boldsymbol{\eta})\boldsymbol{\eta} > 0,\ \forall\,\boldsymbol{\nu},\,\boldsymbol{\eta} \neq 0 \in \mathbb{R}^{6\times1} \tag{12}$$

Property 4. *The vector $\boldsymbol{g}^\star_{\boldsymbol{\eta}}(\boldsymbol{\eta})$ is continuous and bounded if the vehicle's trajectory is smooth and bounded Kelly et al. (2006).*

Property 5. *The saturation bounds of the UUV's actuators can be exploited to upper bound the vehicle's thrusters velocities by a positive constant Tijjani et al. (2021), i.e.*

$$\left|\boldsymbol{\tau}^\star_{\boldsymbol{\eta}}(\boldsymbol{\eta})_i\right| \le \kappa^\star,\ \text{where } i = \overline{1,6}, \kappa^\star \in \mathbb{R}_{>0}. \tag{13}$$

3. Key Tracking Control Schemes Design and their Real-Time Validations

3.1. PD/PID based Control Scheme

In this class, the PID control scheme is selected as a representative control scheme mainly due to the following reasons. It is the most popular control algorithm widely applied in robotic systems, including UUVs. In addition to the simple architecture of the PID control scheme, this control law fulfils the basic control objectives for many real-time applications Guerrero et al. (2019c), Kim et al. (2013). Indeed, most of the advanced control schemes proposed in literature depend implicit or explicitly on some form of the PID philosophy Somefun et al. (2021). Thus, this control scheme is considered as a benchmark in the domain of automatic control.

3.1.1. Basic design principle

The standard PID control algorithm has the following architecture:

$$u(t) = K_p e(t) + K_i \int_0^t e(\sigma) d\sigma + K_d \dot{e}(t) \tag{14}$$

where $u(t)$ defines the control input signal, $e(t)$ is the error signal representing the difference between the desired and output signals, while K_p, K_i, and K_d are respectively the feedback proportional, integral, and derivative gains.
Note that an optimal tuning of these feedback gains is a tedious task. Therefore, a lot of tuning strategies can be found in the literature Tijjani and Chemori (2020). Despite all the success recorded by the PID control scheme and its enhanced versions, non-optimal feedback gains can often result in an unstable behavior of the overall closed-loop dynamics. For further details about the basic design principle of this kind of controllers, the reader can refer to the following key references: Tijjani and Chemori (2021), Hou and Cheah (2011), Ippoliti et al. (2005), Lin et al. (2008), Campos et al. (2017), Wan et al. (2019) etc.).

3.1.2. Application to UUVs tracking control

We proposed to improve the standard PID structure in (14), as well as in Tijjani and Chemori (2021), by adding the desired feedforward dynamics of the vehicle in (9). The main goal of the controller is to guide the vehicle to follow the desired trajectory designed as follows:

$$\boldsymbol{\eta}_d(t) = [x_d(t),\ y_d(t),\ z_d(t),\ \phi_d(t),\ \theta_d(t),\ \psi_d(t)]^T \tag{15}$$

If the vehicle's trajectory is expressed as:

$$\boldsymbol{\eta}(t) = [x(t),\ y(t),\ z(t),\ \phi(t),\ \theta(t),\ \psi(t)]^T \tag{16}$$

The tracking error $\boldsymbol{e}(t)$ and its first time-derivative are computed as follows:

$$\boldsymbol{e}(t) = \boldsymbol{\eta}_d(t) - \boldsymbol{\eta}(t), \quad \dot{\boldsymbol{e}}(t) = \dot{\boldsymbol{\eta}}_d(t) - \dot{\boldsymbol{\eta}}(t) \tag{17}$$

where $\boldsymbol{e}(t) = [e_1(t), e_2(t), \cdots, e_6(t)]^T$ is a vector of the tracking errors, $\dot{\boldsymbol{e}}(t) = [\dot{e}_1(t), \dot{e}_2(t), \cdots, \dot{e}_6(t)]^T$ represents the first time-derivative of $\boldsymbol{e}(t)$, while $\dot{\boldsymbol{\eta}}(t)$ and $\dot{\boldsymbol{\eta}}_d(t)$ are first time-derivatives of the vehicle's ($\boldsymbol{\eta}(t)$) and desired ($\boldsymbol{\eta}_d(t)$) trajectories, respectively.
The vector of the control inputs $\boldsymbol{\tau}$ of the vehicle (*Leonard UUV*) is designed as:

$$\begin{aligned}\boldsymbol{\tau}^\star = \boldsymbol{J}^T(\boldsymbol{\eta})\Big[&\boldsymbol{M}^\star_{\boldsymbol{\eta}}(\boldsymbol{\eta})\ddot{\boldsymbol{\eta}}_d + \boldsymbol{C}^\star_{\boldsymbol{\eta}}(\boldsymbol{\nu},\boldsymbol{\eta})\dot{\boldsymbol{\eta}}_d + \boldsymbol{D}^\star_{\boldsymbol{\eta}}(\boldsymbol{\nu},\boldsymbol{\eta})\dot{\boldsymbol{\eta}}_d \\ &+ \boldsymbol{g}^\star_{\boldsymbol{\eta}}(\boldsymbol{\eta}) + \boldsymbol{K}_p\boldsymbol{e}(t) + \boldsymbol{K}_i\int_0^t \boldsymbol{e}(\sigma)d\sigma + \boldsymbol{K}_d\dot{\boldsymbol{e}}(t)\Big]\end{aligned} \tag{18}$$

where $\boldsymbol{\tau}^\star = [\tau^\star_x,\ \tau^\star_y,\ \tau_z,\ \tau^\star_\phi,\ \tau^\star_\theta,\ \tau^\star_\psi]^T$ defines the vector of the control inputs for the six DOFs. $\boldsymbol{K}_p = diag\{k_{1p}, k_{2p}, ..., k_{6p}\} > 0$, $\boldsymbol{K}_i = diag\{k_{1i}, k_{2i}, ..., k_{6i}\} > 0$, and $\boldsymbol{K}_d = diag\{k_{1d}, k_{2d}, ..., k_{6d}\} > 0$ are the feedback gains matrices. The remaining terms have been defined previously.
The closed-loop stability analysis of this control law and its improved version, implemented on UUV, can be found in Tijjani and Chemori (2020) and Guerrero et al. (2019c), respectively.

3.2. SMC based Control Scheme

Although though a first-order sliding-mode control (SMC) scheme has been noticed for dealing with time-varying disturbances and parametric uncertainties, this approach requires infinite control bandwidths Fischer et al. (2014b), Wang and Su (2021). This problem leads to chattering phenomena. To alleviate the chattering in first-order SMC, a second-order SMC scheme like a Robust Integral of the Sign of the Error (RISE) control has been proposed for UUVs in Fischer et al. (2014b). Based on the real-time experimental results obtained in Fischer et al. (2014b), we proposed to use the RISE controller as our representative control scheme in this class.

3.2.1. Basic design principle

The design of the standard RISE controller for a multiple-input multiple-out (MIMO) system is revisited by considering the following dynamics.

$$\boldsymbol{M}(\boldsymbol{q},\dot{\boldsymbol{q}})\ddot{\boldsymbol{q}}(t) + \boldsymbol{F}(\boldsymbol{q},\dot{\boldsymbol{q}},t) = \boldsymbol{u}(t) \tag{19}$$

where $\boldsymbol{q}(t) \in \mathbb{R}^{n\times 1}$ defines the state of the system with n DOFs and $\boldsymbol{u}(t) \in \mathbb{R}^{n\times 1}$ represents the control input. $\boldsymbol{M}(\boldsymbol{q},\dot{\boldsymbol{q}}) \in \mathbb{R}^{n\times n}$ and $\boldsymbol{F}(\boldsymbol{q},\dot{\boldsymbol{q}},t) \in \mathbb{R}^{n\times 1}$ are the uncertain functions of the dynamic system.
To facilitate the design of the controller, an auxiliary tracking error is computed as follows Xian et al. (2004):

$$\boldsymbol{e}_2(t) = \dot{\boldsymbol{e}}_1(t) + \alpha_1\boldsymbol{e}_1(t) \tag{20}$$

where $\boldsymbol{e}_1(t) = \boldsymbol{q}_d(t) - \boldsymbol{q}(t)$ is the tracking error, $\boldsymbol{q}_d(t)$ is the desired trajectory, $\boldsymbol{q}(t)$ is the system trajectory, $\dot{\boldsymbol{e}}_1(t)$ is the first time-derivative of $\boldsymbol{e}_1(t)$, and $\alpha_1 > 0$ is a positive constant.
Similarly, a second filter tracking error $\boldsymbol{r}(t)$ is designed as a function of (20), subsequently as follows:

$$\boldsymbol{r}(t) = \dot{\boldsymbol{e}}_2(t) + \alpha_2\boldsymbol{e}_2(t) \tag{21}$$

where $\alpha_2 > 0$ is also a positive constant and $\boldsymbol{e}_2(t)$ has been derived in (20), $\dot{\boldsymbol{e}}_2(t)$ is the first time-derivative of $\boldsymbol{e}_2(t)$. Note

that $\boldsymbol{r}(t)$ is not used in the control design. It is only proposed to simplify closed-loop stability analysis.
Finally, the standard RISE controller for the dynamics in (19) is designated as follows:

$$\boldsymbol{u}(t) = (\boldsymbol{k}_s + \boldsymbol{I})\boldsymbol{e}_2(t) - (\boldsymbol{k}_s + \boldsymbol{I})\boldsymbol{e}_2(0) + \int_0^t (\boldsymbol{k}_s + \boldsymbol{I})\alpha_2 \boldsymbol{e}_2(\sigma)d\sigma + \int_0^t \boldsymbol{\beta} sgn(\boldsymbol{e}_2(\sigma))d\sigma \tag{22}$$

Note that the system's initial condition is assumed to be zero. Otherwise, the controller requires an initial condition. Where $\boldsymbol{k}_s = diag\{k_{s1}, k_{s2}, \cdots, k_{sn}\}$ and $\boldsymbol{\beta} = diag\{\beta_1, \beta_2, \cdots, \beta_n\}$ are the matrices containing the controller's parameters. $\boldsymbol{I} = diag\{I_1, I_2, \cdots, I_n\}$ is an identity matrix and sgn is the standard sigmoid function (For more details on the basic design principle of this kind of control laws, the reader can refer to the following main references: Xian et al. (2004), Fischer et al. (2014b), Wang and Su (2021), etc.).

3.2.2. *Application to UUVs tracking control*

Even though the standard RISE controller is a non-model-based scheme, inspired from Fischer et al. (2014b), we propose to compensate the dynamics of the vehicle in the control architecture. Hence, the RISE control scheme is designed as follows:

$$\begin{aligned}\boldsymbol{\tau}^\star = \boldsymbol{J}^T(\boldsymbol{\eta})\Big[&\boldsymbol{M}^\star_{\boldsymbol{\eta}}(\boldsymbol{\eta})\ddot{\boldsymbol{\eta}}_d + \boldsymbol{C}^\star_{\boldsymbol{\eta}}(\boldsymbol{\nu},\boldsymbol{\eta})\dot{\boldsymbol{\eta}}_d + \boldsymbol{D}^\star_{\boldsymbol{\eta}}(\boldsymbol{\nu},\boldsymbol{\eta})\dot{\boldsymbol{\eta}}_d \\ &+(\boldsymbol{K}_s + \boldsymbol{I})\boldsymbol{e}^\star_1(t) - (\boldsymbol{K}_s + \boldsymbol{I})\boldsymbol{e}^\star_1(0) + \int_0^t (\boldsymbol{K}_s + \boldsymbol{I}) \\ &\times\alpha_2 \boldsymbol{e}^\star_1(\sigma)d\sigma + \int_0^t \boldsymbol{\beta}^\star sgn(\boldsymbol{e}^\star_1(\sigma))d\sigma\Big]\end{aligned} \tag{23}$$

where $\boldsymbol{e}^\star_1(t) = \dot{\boldsymbol{e}}(t) + \alpha_1 \boldsymbol{e}(t)$. $\boldsymbol{K}_s = diag\{K_{s1}, K_{s2}, \cdots, K_{s6}\}$ and $\boldsymbol{\beta}^\star = diag\{\beta^\star_1, \beta^\star_2, \cdots, \beta^\star_6\}$ are the gains matrices. $\boldsymbol{e}(t)$ and $\dot{\boldsymbol{e}}(t)$ have been defined in (17). $\boldsymbol{I} = diag\{I_1, I_2, \cdots, I_6\}$ is an identity matrix, while the remaining terms have been defined previously.

Remark 6. *It is worth noting that despite the implementation simplicity of the standard RISE control scheme, its stability analysis is not a trivial task. The detail stability study of this controller implemented on a UUV can be found in Fischer et al. (2014b).*

3.3. Adaptive based Control Scheme

It is well-known that having partial/complete knowledge of the UUV's dynamics enhances the effectiveness of a tracking controller. On the other hand, this dynamics is always difficult to obtain a priori. To deal with this critical issue, an adaptive control scheme has been proposed as one of the ultimate solutions. The fundamental design technique of this scheme is given subsequently.

3.3.1. *Basic design principle*

Since most of the robotic system has the linearity property in terms of their parameters, this quality is often exploited in adaptive control design Antonelli et al. (2001). Based on this notion, the six DOFs dynamics of robotic systems can be generally represented as follows:

$$\boldsymbol{\Gamma} = \boldsymbol{\Phi}(\cdot)\boldsymbol{\vartheta} \tag{24}$$

where $\boldsymbol{\Gamma} \in \mathbb{R}^{n\times1}$ is the vector of the control inputs, $\boldsymbol{\Phi}(\cdot) \in \mathbb{R}^{n\times n_\vartheta}$ is a regressor matrix containing the known part of the system's dynamics, and $\boldsymbol{\vartheta} \in \mathbb{R}^{n_\vartheta\times1}$ is the vector of the unknown dynamic parameters.
From (24), an adaptive law can be designed to update the dynamics online. Next, a feedback control algorithm is added to achieve the control objectives (For further details about the basic design principle of this kind of controllers, the reader can refer to the following key references: Antonelli et al. (2001), Saied et al. (2019), Fischer et al. (2014a), Maalouf et al. (2015b), etc.).

3.3.2. *Application to UUVs tracking control*

Inspired by Antonelli et al. (2001), the UUV dynamics in (9) can be expressed as:

$$\boldsymbol{\Phi}(\ddot{\boldsymbol{\eta}}, \dot{\boldsymbol{\eta}}, \boldsymbol{\eta}, \boldsymbol{\nu})\underline{\boldsymbol{\vartheta}} = \boldsymbol{\tau}^\star_{\boldsymbol{\eta}}(\boldsymbol{\eta}) + \boldsymbol{w}^\star_{\boldsymbol{\eta}}(t) \tag{25}$$

where $\boldsymbol{\Phi}(\cdot) \in \mathbb{R}^{6\times n_{\underline{\vartheta}}}$ is a regressor matrix and $\underline{\boldsymbol{\vartheta}} \in \mathbb{R}^{n_{\underline{\vartheta}}\times1}$ is the vector of the dynamic parameters.
Based on (25), the adaptive control scheme for the vehicle is designed as follows:

$$\boldsymbol{\tau}^\star = \boldsymbol{J}^T(\boldsymbol{\eta})\Big[\boldsymbol{\Phi}(\ddot{\boldsymbol{\eta}}_d, \dot{\boldsymbol{\eta}}_d, \boldsymbol{\eta}_d)\hat{\underline{\boldsymbol{\vartheta}}} + \underline{\boldsymbol{K}}_p \boldsymbol{e}(t) + \underline{\boldsymbol{K}}_d \dot{\boldsymbol{e}}(t)\Big] \tag{26}$$

To improve the efficiency of this control scheme, the desired trajectories are used instead of the acquired ones from the vehicle's sensors. It is worth to note that the dynamic parameters are estimated based on the tracking error. These parameters are update online using an adaptation law design as follows:

$$\dot{\hat{\underline{\boldsymbol{\vartheta}}}} = \underline{\boldsymbol{K}}^{-1}_{\boldsymbol{\vartheta}} \boldsymbol{\Phi}^T(\cdot)[\dot{\boldsymbol{e}}(t) + \Lambda \boldsymbol{e}(t)] \tag{27}$$

where $\dot{\hat{\underline{\boldsymbol{\vartheta}}}}$ is the first time-derivative of $\boldsymbol{\vartheta}$, $\Lambda > 0$, and $\underline{\boldsymbol{K}}^{-1}_{\boldsymbol{\vartheta}} = diag\{\underline{k}_1, \underline{k}_2, \cdots, \underline{k}_6\}$ is the adaptation gain matrix. $\underline{\boldsymbol{K}}_p = diag\{\underline{k}_{p1}, \underline{k}_{p2}, \cdots, \underline{k}_{p6}\}$ and $\underline{\boldsymbol{K}}_d = diag\{\underline{k}_{d1}, \underline{k}_{d2}, \cdots, \underline{k}_6\}$ are the feedback gains. $\boldsymbol{e}(t)$ and $\dot{\boldsymbol{e}}(t)$ have been defined in (17), while the remaining terms have been defined previously. Further details on how to design the matrix $\boldsymbol{\Phi}(\cdot)$ can be found in Tijjani and Chemori (2020), Antonelli et al. (2001), and Saied et al. (2019).

3.4. Observation-based Control Scheme

The main challenge always faced in the automatic control community is how to obtain full-state measurements when designing a controller. In fact, most of the control schemes in the literature are designed based on the assumption that the full-state measurements of the dynamical systems are accessible. As discussed previously, from the practical perspective, this assumption may not be true always. To deal with this critical issue of the full-state measurements, state observers are proposed for the full-state estimation of many physical systems Zemouche et al. (2019), Ajwad et al. (2019). One of the famous observer structures in the literature is the high gain observer (HGO) due to its ability to estimate online the time derivatives of the outputs Esfandiari and Khalil (1992). Similarly, we consider HGO as our representative observer in this work.

3.4.1. Basic design principle

To demonstrate briefly the design of HGO, let us first consider the following second-order nonlinear dynamics.

$$\begin{cases} \dot{\underline{x}}_1 = \underline{x}_2 & \underline{x}_1(0) = \underline{x}_{10} \\ \dot{\underline{x}}_2 = \underline{\phi}^\star(\underline{x}_2, \underline{x}_1, \underline{u}, \underline{\chi}) & \underline{x}_2(0) = \underline{x}_{20} \\ \underline{y} = \underline{x}_1 \end{cases} \tag{28}$$

where $(\underline{x}_2, \underline{x}_1)$ are the system's states, $\underline{u}$ is a vector of the control inputs, $(\underline{x}_2(0), \underline{x}_1(0))$ denote the initial conditions, $\underline{\chi}$ represents a time-varying external disturbance, and y is the output of the dynamic system.
Based on the assumption that the dynamics (28) is controllable by the state feedback controller $\underline{u} = \underline{\gamma}(\underline{x}_2, \underline{x}_1)$, the HGO can be designed to provide the states $(\underline{x}_2, \underline{x}_1)$ estimations to this controller as follows:

$$\begin{aligned} \dot{\hat{\underline{x}}}_1 &= \hat{\underline{x}}_2 + \underline{h}_1(\underline{y} - \hat{\underline{x}}_1) \\ \dot{\hat{\underline{x}}}_2 &= \underline{\phi}_0(\hat{\underline{x}}_2, \hat{\underline{x}}_1, \underline{\gamma}(\hat{\underline{x}}_2, \hat{\underline{x}}_1)) + \underline{h}_2(\underline{y} - \hat{\underline{x}}_1) \end{aligned} \tag{29}$$

where $(\hat{\underline{x}}_2, \hat{\underline{x}}_1)$ are the estimates of $(\underline{x}_2, \underline{x}_1)$, respectively. $\underline{\gamma}(\cdot)$ is the control law. $\underline{\phi}_0(\hat{\underline{x}}_2, \hat{\underline{x}}_1, \underline{\gamma}(\hat{\underline{x}}_2, \hat{\underline{x}}_1))$ represents the nominal model of the $\underline{\phi}^\star(\hat{\underline{x}}_2, \hat{\underline{x}}_1, \underline{\gamma}(\hat{\underline{x}}_2, \hat{\underline{x}}_1))$ and $(\underline{h}_1, \underline{h}_2)$ are the observer gains.
At this point, the estimation error dynamics (difference between (29) and (28)) is expressed as follows:

$$\begin{aligned} \dot{\tilde{\underline{x}}}_1 &= \tilde{\underline{x}}_2 - \underline{h}_1 \tilde{\underline{x}}_1 \\ \dot{\tilde{\underline{x}}}_2 &= \underline{\phi}(\hat{\underline{x}}_2, \hat{\underline{x}}_1, \underline{x}_2, \underline{x}_1, \underline{\chi}) - \underline{h}_2 \tilde{\underline{x}}_1 \end{aligned} \tag{30}$$

where $\underline{\phi} = \underline{\phi}^\star(\underline{x}_2, \underline{x}_1, \underline{\gamma}(\underline{x}_2, \underline{x}_1), \underline{\chi}) - \underline{\phi}_0(\hat{\underline{x}}_2, \hat{\underline{x}}_1, \underline{\gamma}(\hat{\underline{x}}_2, \hat{\underline{x}}_1))$.
To ensure the fast decay of $\tilde{\underline{x}}_1$ and $\tilde{\underline{x}}_2$, the gains $\underline{h}_1$ and $\underline{h}_2$ should be designed as the observer high gains, which is demonstrated as follows:

$$\underline{h}_1 = \frac{c_1}{E}, \quad \underline{h}_1 \quad = \frac{c_2}{E^2} \tag{31}$$

where $(c_1 > 0, c_2 > 0)$ are designed parameters and $E > 0$ is a positive constant (with a small value).
Next, (30) can be transformed and redefined as follows:

$$\begin{aligned} E\dot{g}_1 &= g_2 - c_1 g_1 \\ E\dot{g}_2 &= E\underline{\phi} - c_2 g_1 \end{aligned} \tag{32}$$

where $g_1 = \frac{\tilde{x}_1}{E}$ and $g_2 = \tilde{\underline{x}}_2$. It is worth noting that making the numerical value of the parameter E very close to the zero suppresses the negative effects of disturbances in $\underline{\phi}$. On the other hand, the error dynamics will become faster compared to the system's dynamics (28); this always results in the peaking problem (For more details concerning the basic design principle of this kind of observers, as well as their peaking problems, the reader can refer to the following main references: Khalil (2008), Khalil and Praly (2014), Dabroom and Khalil (2001), etc.).

3.4.2. Application to UUVs tracking control

We propose that the selected HGO should work in tandem with a generalized super-twisting controller (GSTC). The main reason is due to the effectiveness demonstrated by the controller in several real-time validations from the literature (see for instance, Borlaug et al. (2021), Guerrero et al. (2019b), Borlaug et al. (2021), etc.). Additionally, the closed-loop stability analysis of this controller is well-established. To facilitate the observer/control scheme development, first, the vehicle's dynamics in (20) is expressed in the so-called state-space form, as follows:

$$\begin{cases} \dot{\underline{\boldsymbol{\eta}}}(t) = \boldsymbol{A}_{\underline{\boldsymbol{\eta}}(t)} \underline{\boldsymbol{\eta}}(t) + \boldsymbol{B}_{\underline{\boldsymbol{\eta}}(t)} \boldsymbol{u}(t) + \boldsymbol{D}\dot{\underline{\boldsymbol{w}}}^\star_{\boldsymbol{\eta}}(t) \\ \boldsymbol{y}(t) = \boldsymbol{C}\underline{\boldsymbol{\eta}}(t) \end{cases} \tag{33}$$

where $\underline{\boldsymbol{\eta}}(t) = [\boldsymbol{\eta}(t)^T \ \dot{\boldsymbol{\eta}}(t)^T]^T$, $\boldsymbol{A}_{\underline{\boldsymbol{\eta}}(t)} = \begin{bmatrix} \boldsymbol{0}_{6\times6} & \boldsymbol{I}_{6\times6} \\ \boldsymbol{0}_{6\times6} & -[\boldsymbol{M}^\star_{\boldsymbol{\eta}}(\boldsymbol{\eta})]^{-1} \end{bmatrix}$, $\boldsymbol{B}_{\underline{\boldsymbol{\eta}}(t)} = \begin{bmatrix} \boldsymbol{0}_{6\times6} \\ [\boldsymbol{M}^\star_{\boldsymbol{\eta}}(\boldsymbol{\eta})]^{-1} \end{bmatrix}$, $\underline{\boldsymbol{w}}^\star_{\boldsymbol{\eta}}(t) = \boldsymbol{w}^\star_{\boldsymbol{\eta}}(t) + \dot{\boldsymbol{\eta}}(t) - \boldsymbol{C}^\star_{\boldsymbol{\eta}}(\boldsymbol{\nu}, \boldsymbol{\eta})\dot{\boldsymbol{\eta}} - \boldsymbol{D}^\star_{\boldsymbol{\eta}}(\boldsymbol{\nu}, \boldsymbol{\eta})\dot{\boldsymbol{\eta}} - \boldsymbol{g}^\star_{\boldsymbol{\eta}}(\boldsymbol{\eta})$, $\boldsymbol{D} = \begin{bmatrix} \boldsymbol{0}_{6\times6} & [\boldsymbol{M}^\star_{\boldsymbol{\eta}}(\boldsymbol{\eta})]^{-1} \end{bmatrix}^T$, $\boldsymbol{u}(t) = \boldsymbol{\tau}^\star_{\boldsymbol{\eta}}(\boldsymbol{\eta})$, $\boldsymbol{y}(t)$ is the output vector, $\boldsymbol{C}$ is the output matrix, and the dynamics terms have been previously defined. Note that the dimensions of $\boldsymbol{y}(t)$ and $\boldsymbol{C}$ depend on the number of sensors installed on the vehicle.
Also, the matrix $\boldsymbol{A}_{\underline{\boldsymbol{\eta}}(t)}$ can be easily transformed into the triangular structure. Then, the whole dynamics is rewritten in an extended state-space form as:

$$\begin{cases} \dot{\bar{\underline{\boldsymbol{\eta}}}}(t) = \bar{\boldsymbol{A}}_{\bar{\underline{\boldsymbol{\eta}}}(t)} \bar{\underline{\boldsymbol{\eta}}}(t) + \bar{\boldsymbol{B}}_{\bar{\underline{\boldsymbol{\eta}}}(t)} \boldsymbol{u}(t) + \bar{\boldsymbol{D}}\bar{\boldsymbol{w}}(t) \\ \bar{\boldsymbol{y}}(t) = \bar{\boldsymbol{C}}\bar{\underline{\boldsymbol{\eta}}}(t) \end{cases} \tag{34}$$

where $\bar{\underline{\boldsymbol{\eta}}}(t) = [\underline{\boldsymbol{\eta}}(t)^T \ \underline{\boldsymbol{w}}^\star_{\boldsymbol{\eta}}(t)^T]^T$, $\bar{\boldsymbol{A}} = \begin{bmatrix} \boldsymbol{A} & \boldsymbol{D} \\ \boldsymbol{0}_{6\times12} & \boldsymbol{0}_{6\times6} \end{bmatrix}$, $\bar{\boldsymbol{B}} = \begin{bmatrix} \boldsymbol{B} & \boldsymbol{0}_{6\times6} \end{bmatrix}^T$, $\bar{\boldsymbol{D}} = \begin{bmatrix} \boldsymbol{0}_{6\times6} & \boldsymbol{D} \end{bmatrix}^T$, $\bar{\boldsymbol{C}} = \begin{bmatrix} \boldsymbol{C} & \boldsymbol{0}_{6\times6} \end{bmatrix}$, and $\bar{\boldsymbol{w}}(t) = \dot{\underline{\boldsymbol{w}}}^\star_{\boldsymbol{\eta}}(t)$.

Remark 7. *The term $\boldsymbol{w}^\star_{\boldsymbol{\eta}}(t)$ is a continuous Lipschitz function. The vehicle's dynamics and this function are bounded based on the dynamic properties discussed in Section II. This also means that $\underline{\boldsymbol{w}}^\star_{\boldsymbol{\eta}}(t)$ and $\dot{\underline{\boldsymbol{w}}}^\star_{\boldsymbol{\eta}}(t)$ are assumed to be smooth and bounded.*

Inspired from the HGO developed in Atassi and Khalil (2000), we extend and design the same structure to UUV dynamics in (34), as follows:

$$\dot{\hat{\bar{\underline{\boldsymbol{\eta}}}}}(t) = \bar{\boldsymbol{A}}_{\hat{\bar{\underline{\boldsymbol{\eta}}}}(t)} \hat{\bar{\underline{\boldsymbol{\eta}}}}(t) + \bar{\boldsymbol{B}}_{\hat{\bar{\underline{\boldsymbol{\eta}}}}(t)} \boldsymbol{u}(t) + \boldsymbol{H}(\boldsymbol{y}(t) - \bar{\boldsymbol{C}}\hat{\bar{\underline{\boldsymbol{\eta}}}}(t)) \tag{35}$$

where $\underline{\hat{\boldsymbol{\eta}}}(t)$ is a vector of the estimated states by the HGO, $\dot{\underline{\hat{\boldsymbol{\eta}}}}(t)$ is a vector of the first time-derivative of $\underline{\hat{\boldsymbol{\eta}}}(t)$, and $\boldsymbol{H} = diag\{H_1, H_2, \cdots, H_{18}\}$ is a diagonal matrix of the high-gain parameters of the HGO. Each element of the matrix $\boldsymbol{H}$ is designed as $H_j = \frac{h_j}{\epsilon^j}$, where $j = \overline{1, 18}$.
For the case of the controller design, let us consider the sliding surface of the controller as,

$$\boldsymbol{\sigma}(t) = \underline{\dot{\boldsymbol{e}}}(t) + \underline{\boldsymbol{\Lambda}}\underline{\boldsymbol{e}}(t) \tag{36}$$

where $\underline{\boldsymbol{e}}(t) = \boldsymbol{\eta}_d(t) - \underline{\hat{\boldsymbol{\eta}}}(t)$ and $\underline{\dot{\boldsymbol{e}}}(t) = \dot{\boldsymbol{\eta}}_d(t) - \dot{\underline{\hat{\boldsymbol{\eta}}}}(t)$. Note that the controller uses the states (i.e. $\underline{\hat{\boldsymbol{\eta}}}(t), \dot{\underline{\hat{\boldsymbol{\eta}}}}(t)$) estimated by the HGO. $\boldsymbol{\sigma}(t) = [\sigma_1, \sigma_2, \cdots, \sigma_6]^T$ is a vector of the sliding surface, $\underline{\boldsymbol{\Lambda}} = diag\{\underline{\Lambda}_1, \underline{\Lambda}_2, \cdots, \underline{\Lambda}_6\}$ is a positive definite matrix
Next, the GSTC is designed for the six DOFs of the vehicle as follows:

$$\boldsymbol{\tau}^\star = \boldsymbol{J}^T(\underline{\hat{\boldsymbol{\eta}}})\boldsymbol{M}^\star_{\underline{\hat{\boldsymbol{\eta}}}}(\underline{\hat{\boldsymbol{\eta}}})[\ddot{\boldsymbol{\eta}}_d(t) + \boldsymbol{\Lambda}\dot{\boldsymbol{e}}(t) - \boldsymbol{F}(\underline{\hat{\boldsymbol{\eta}}}) - \underline{\boldsymbol{\nu}}] \tag{37}$$

where $\boldsymbol{F}(\underline{\hat{\boldsymbol{\eta}}}) = -[\boldsymbol{M}^\star_{\underline{\hat{\boldsymbol{\eta}}}}(\underline{\hat{\boldsymbol{\eta}}})]^{-1}[\boldsymbol{C}^\star_{\underline{\hat{\boldsymbol{\eta}}}}(\hat{\boldsymbol{\nu}}, \underline{\hat{\boldsymbol{\eta}}})\dot{\underline{\hat{\boldsymbol{\eta}}}}(t) + \boldsymbol{D}^\star_{\underline{\hat{\boldsymbol{\eta}}}}(\hat{\boldsymbol{\nu}}, \underline{\hat{\boldsymbol{\eta}}})\dot{\underline{\hat{\boldsymbol{\eta}}}}(t) + \boldsymbol{g}^\star_{\underline{\hat{\boldsymbol{\eta}}}}(\underline{\hat{\boldsymbol{\eta}}})]$, and $\underline{\boldsymbol{\nu}}$ is expressed as:

$$\underline{\boldsymbol{\nu}} = -\boldsymbol{K}^\star_1\boldsymbol{\Psi}_1(\boldsymbol{\sigma}) + \boldsymbol{\lambda} \tag{38}$$

Then, $\boldsymbol{\lambda}$ is given as:

$$\boldsymbol{\lambda} = -\boldsymbol{K}^\star_2\boldsymbol{\Psi}_2(\boldsymbol{\sigma}) \tag{39}$$

By considering a scalar case, the elements of the $\boldsymbol{\Psi}_1(\boldsymbol{\sigma})$ and $\boldsymbol{\Psi}_2(\boldsymbol{\sigma})$ are formulated as follows:

$$\begin{aligned} \Psi_{1i}(\sigma_i) &= \mu_{1i}\left|\sigma_i\right|^{0.5} sgn(\sigma_i) + \mu_{2i}\sigma_i, \qquad i = \overline{1,6} \\ \Psi_{2i}(\sigma_i) &= \frac{1}{2}\mu_{1i}^2 sgn(\sigma_i) + \frac{3}{2}\mu_{1i}\mu_{2i}\left|\sigma_i\right|^{0.5} sgn(\sigma_i) + \mu_{2i}^2\sigma_i \end{aligned} \tag{40}$$

with $\mu_{1i} \geq 0$, $\mu_{2i} \geq 0$, $\boldsymbol{K}^\star_1 = diag\{k^\star_{11}, k^\star_{12}, \cdots, k^\star_{16}\}$, and $\boldsymbol{K}^\star_2 = diag\{k^\star_{21}, k^\star_{22}, \cdots, k^\star_{26}\}$. The remaining terms have been defined previously.

3.5. Combined Control Scheme for UUVs Tracking

To clearly demonstrate the idea of a combined control scheme in a simple way, we propose to adapt the feedforward dynamics of the observer/controller scheme designed in the previous class as follows:

$$\boldsymbol{\tau}^\star = \boldsymbol{J}^T(\underline{\hat{\boldsymbol{\eta}}})[\boldsymbol{\Phi}(\ddot{\boldsymbol{\eta}}_d, \dot{\boldsymbol{\eta}}_d, \boldsymbol{\eta}_d)\underline{\hat{\boldsymbol{\vartheta}}} + \boldsymbol{\Lambda}\dot{\boldsymbol{e}}(t) - \underline{\boldsymbol{\nu}}] \tag{41}$$

where all the terms in (41) have been designed using the same methodology applied in the adaptive based control scheme as well as the approach used in the observation-based class (For further details about the basic design principle of this type of control algorithms, the reader can refer to the following key references: Miao et al. (2013), Qiu et al. (2021), Jiang et al. (2021), Zhu et al. (2021), Qiao and Zhang (2019), Xu et al. (2015), etc.).

Table 2
Main Technical Specifications of *Leonard UUV*

Components	Specifications/Descriptions
Attitude Sensor	Sparkfun MPU 9250, MEMS 9-axes gyrometer, accelerometer and magnetometer microprocessor.
Depth Sensor	Pressure sensor MS5803-02BA.
Dimensions	75cm (L) × 55cm (W) × 45cm (H).
Sampling Periods	Attitude sensor = 40ms and Depth sensor = 50ms.
Computing Resource	Dell Latitude E6230 Intel Core i7 - 2.9 GHz, 16 GB of RAM, 64 bits Windows 10 OS, Microsoft Visual C++ 2015.
Floatability	9N.
Mass	28kg.
Maximal Depth	100m (range depending on the depth sensor).
Power Consumption	24V, 600W.
Tether	50m in pool configuration.
Thrusters	6-Seabotix BTD150 continuous thrust 2.2kgf each with Syren 10 drivers.

3.6. Autonomous Vehicle Description

The representative control schemes in this survey, designed previously in this section, are implemented and carefully compared in real-time using a fully actuated vehicle named *Leonard UUV*. This vehicle is one of the UUVs available at LIRMM, University of Montpellier, CNRS. The technical aspects of *Leonard UUV* have been described in Tijjani et al. (2021). In this survey, we propose to revisit some of these technical features to point out another challenging issue that affects the performance of autonomous control algorithms for UUVs in real-time marine missions. *Leonard UUV* has six independent thrusters, which make the vehicle highly maneuverable when operating either in autonomous or shared control mode with a remote human pilot. Furthermore, in the design of this vehicle, the positions of its two centers (i.e. buoyancy and gravity) coincide in order to stabilize both the roll (ϕ) and the pitch (θ) angles around zero naturally (i.e. $\phi \approx \theta \approx 0$). Additionally, keeping these angles close to zero minimizes the vehicle's energy consumption. Furthermore, the vehicle uses two sensors for depth and attitude measurements, as described in TABLE 2. We can observe that in TABLE 2, the sensors have *different sampling frequencies*; these characteristics of the sensors may negatively affect the performance of the observer/control algorithm implemented on this vehicle.

Remark 8. *Note that some of the above features of this vehicle may simplify or complicate the control design for the vehicle. For this reason, in this survey, we focus on real-time validation and critical evaluation of each representative controller's ability to stabilize the vehicle around the desired position and attitude autonomously.*

3.7. Summary of the Main Implementation Issues

Although we addressed the theoretical design of the six DOFs of the representative controllers previously, for performance evaluation in real-time validation, without loss of generality, we will focus on the autonomous control of two DOFs of the vehicle, that is,

- *The depth.* This DOF represents the vertical translational motion of the vehicle.
- *The yaw.* This DOF describes the heading of the vehicle.

Remark 9. *Note that the vehicle is not equipped with sophisticated sensors like DVL to provide real-time measurements of the surge x and the sway y transnational speeds. In most low-cost commercially available UUVs, these DOFs are either not measured or controlled in open-loop, due to the expensive cost of the DVL sensor.*

Additionally, in many marine tasks, the UUVs need to precisely follow the desired depth and the desired heading as accurate as possible, that is, with zero or minimal error Campos et al. (2017).

For all these reasons, in our real-time validation approach, we carefully access all the representative controllers' ability to maintain the vehicle's trajectories within the vicinity of the desired trajectories. Also, these real-time experiments can serve as a benchmark to select the most suitable control scheme for UUVs operating in different marine conditions. It is worth noting that the efficiency of most of the control algorithms, when deployed to UUVs for real-time applications, is significantly degraded, caused by many factors like the effects of the unmodelled dynamics, internal/external disturbances, parametric uncertainties, and unpredictable operating environments. The scenarios-based real-time experiments proposed, in this survey, are conducted in a laboratory-scale testing pool at LIRMM, depicted in Fig. 3. All the proposed representative controllers are implemented on *Leonard UUV* using C++ in Visual Studio 2015 IDE. The C++ codes for the representative controllers are written using a laptop computer having Intel Core i7-5600U 2.6 GHz CPU, 16 GB of memory (RAM) and Windows 10 as its operating system. These control laws are computed and sent to the propulsion system based on signals acquired from the vehicle's sensors (i.e. depth, inertial measurement unit IMU).

3.8. Proposed Real-Time Experimental Scenarios

To evaluate the performance of all the representative controllers in terms of tracking precision, energy consumption, and robustness, we propose to test the following scenarios in real-time for trajectories (illustrated in Fig. 4) tracking tasks:

Scenario 1 (Nominal Case): The main motivation of this scenario is to tune the feedback gains of each representative controller online for a fair comparative study. The gains of each controller which produce the best tracking performance are maintained for all the subsequent tests. It is worth noting that, in this experiment, the *Leonard UUV* is not subjected to any external perturbations; however the controller performance may be affected by the sensors' measurement noise of the vehicle.

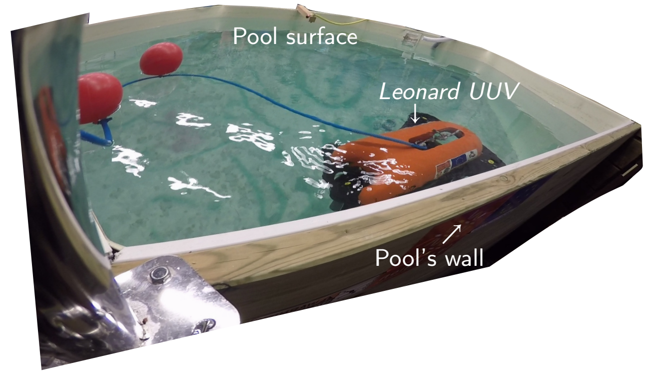

Figure 3: An illustrative view of the our $4m \times 4m \times 1.5m$ testing pool. In the present condition, the *Leonard UUV*, inside the pool, is resting and floating with its natural buoyancy.

Scenario 2 (Robustness Towards Parametric Variations): In this experiment, the robustness of each representative control algorithm is assessed subject to variation in damping and buoyancy (as illustrated in Fig. 5) while performing the task of tracking the desired trajectories.

Scenario 3 (External Disturbances Rejection): This experiment is proposed to investigate how the tracking precision of the representative controllers is affected for real-life tasks such as loading an object (e.g. tool, sample, etc.) and dropping it at a specific desired depth, as demonstrated in Fig. 6. Furthermore, this test will show how the controllers reject a sudden change in the vehicle's weight.

3.9. Real-Time Experimental Comparative Study

In order to study and compare all the five selected representative control schemes, we propose to reassess the efficiency of these control schemes (i.e. model-based PID, **MBPID** is an enhanced version of the controller proposed in Tijjani and Chemori (2021); model-based RISE, **MBRISE** is a slight improvement of the control scheme developed in Fischer et al. (2014b); adaptive model-based PD, **AMPD** is a modification of the control law implemented in Antonelli et al. (2001); observation-based GSTC, **OBS-GSTC** is a model-based observer/GSTC designed in Borlaug et al. (2021); and observation-based adaptive GSTC, **OBS-AGSTC**) in terms of robustness towards parametric uncertainties, time-varying external disturbances rejection, and energy consumption in real-time marine applications as follows.

3.9.1. Obtained Results of Scenario 1 (Nominal Case)

In this real-time mission, the vehicle is used for a tracking task with predefined desired trajectories displayed in Figure 7 (top plots). Note that the vehicle follows these trajectories simultaneously. Focusing first on the depth DOF, the vehicle moves to the desired depth of 0.3 m w.r.t our

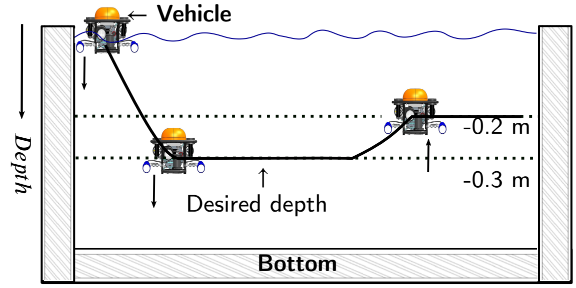

(A)

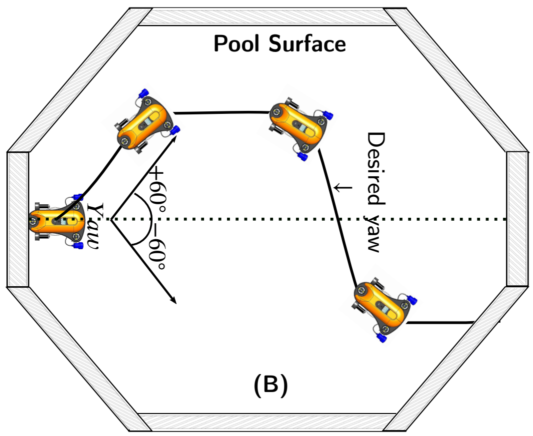

(B)

Figure 4: An illustration of the time-varying predefined desired trajectories (i.e. (A) desired depth and (B) desired yaw) propose to evaluate the performance of the representative control schemes for the tracking tasks using *Leonard UUV*.

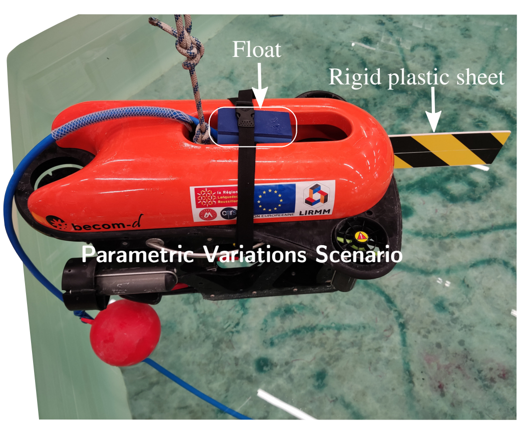

Figure 5: Illustration of a simple reconfiguration of the vehicle for robustness towards uncertainties test: a float and a rigid plastic sheet are fixed to the vehicle in order to increase the buoyancy (by +50%) and the rotational drag on the yaw (by +90%), respectively.

testing pool's surface and stabilizes at this position for about 35 seconds. Then, it goes vertically upwards to a new desired depth of 0.2 m w.r.t the surface and stays there until the end of the mission. For the case of the vehicle's attitude, it turns from its initial yaw of approximately 0° to the desired one set around +60°. After maintaining this orientation for around 33 seconds, the heading of the vehicle is reset to −60°

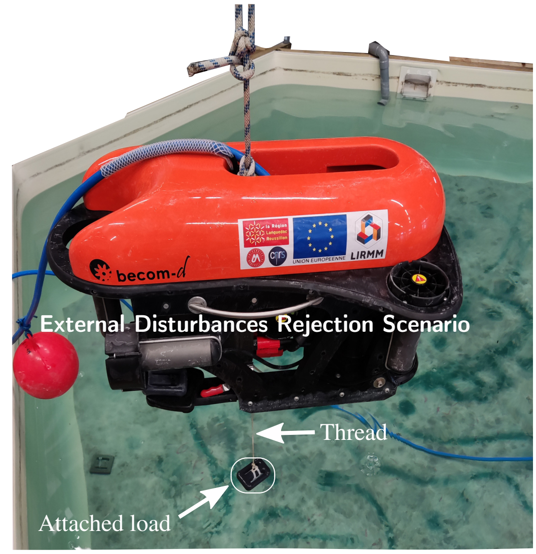

Figure 6: Demonstration of the external disturbances rejection scenario in a real-time experiment: a load is attached to the base of the vehicle with a light thread, which abruptly changes the vehicle's weight during the tracking task.

till the end of this mission. Based on the main goal of this test, highlighted previously, the control parameters giving the best trackings for each controller are kept the same in the subsequent missions; this will ensure a fair comparison of all the five representative control schemes. From Fig. 7 (top left plot), we can quickly observe that the two observation-based schemes (i.e. **OBS-GSTC** and **OBS-AGSTC**) compensate for the dynamic of the vehicle and converge to the desired trajectories. Although the **MBPID** and **AMPD** also converge faster, they oscillate around the desired depth and diverge slightly compared to the **OBS-GSTC** and **OBS-AGSTC** schemes. On the other hand, the yaw trackings of the **OBS-GSTC** and the **OBS-AGSTC** schemes are highly affected by the vehicle's tether drag, caused by the observer error combined with the tracking error. In fact, the yaw tracking of the **OBS-AGSTC** is slightly higher, caused by the sensitivity of the yaw measurement as well as the time taken for the adaptation to counteract the effect of the time-varying dynamics of the vehicle. Also, the tracking performance of the **MBRISE** is good. Moreover, this controller neutralized the negative effect of the tether's drag from the beginning of the mission. Note that the main drawback of all the non-observation-based schemes is that they need full-states measurements. Even though the observation-based schemes are slightly prone to the tether's drag, they outperformed all the remaining controllers in terms of depth tracking. This claim is confirmed by Fig. 7 (middle left plot) as well as the numerical quantification (summarized in Table 3 and Fig. 10) of the tracking errors using root mean square error (RMSE) criterion, given in (42) as follows:

$$RMS[\boldsymbol{e}(t)]_{vehicle's\ position/attitude} = \left[\frac{1}{T_f}\int_0^{T_f} \|\boldsymbol{e}(t)\|^2\, dt\right]^{\frac{1}{2}}$$

(42)

where $\boldsymbol{e}(t)$ has been defined in (17) and T_f represents the period of the real-time mission.

The obtained results clearly show how a careful combination of two or more control schemes can enhance tracking precision and reduce the expensive cost of sensors.

Concerning the control inputs, one can notice chattering free signals for the case of **MBPID** and **MBRISE** according to the bottom plots of Fig. 7. A slight chattering is observed in the control inputs of both the **OBS-GSTC** and the **OBS-AGSTC**, as depicted in Fig. 7 (bottom plots displaying the evolution of the control inputs versus time). For the **AMPD**, the control signals oscillate (around $[2, -3.5]$ N for the depth and between $[-0.1, -0.3]$ Nm for the yaw). Besides better depth tracking, the **OBS-AGSTC** is among the controllers that consume less energy. We numerically quantify the control efforts of all the representative controllers using the integral of control inputs index (INT), expressed mathematically as:

$$INT[\boldsymbol{\tau}]_{vehicle's\ position/attitude} = \int_{t_i}^{t_f} \|\boldsymbol{\tau}(t)\|^2 \, dt \quad (43)$$

where $\boldsymbol{\tau}(t)$ has been defined in (18). t_i and t_f are the initial and final times of the mission, respectively.

It is worth noting that all the control inputs of representative controllers stay within the admissible limit of the vehicle's actuators. A summary of the obtained computational results of the INT index for all the controllers is given in TABLE 4.

3.9.2. *Obtained Results of Scenario 2 (Robustness Towards Damping and Buoyancy Changes)*

To introduce parametric variation in the dynamics presented in (9), we reconfigure our vehicle using a simple technique, illustrated in Figure 5. From the same figure, the rigid plastic sheet (0.45 m × 0.1 m) changes the rotational drag along the yaw axis; thus, increasing the magnitude of the matrix $\boldsymbol{D}^{\star}_{\boldsymbol{\eta}}(\cdot)$ to $\boldsymbol{D}^{\star}_{\boldsymbol{\eta}}(\cdot) + \Delta\boldsymbol{D}^{\star}_{\boldsymbol{\eta}}(\cdot)$ ($\Delta\boldsymbol{D}^{\star}_{\boldsymbol{\eta}}(\cdot) = +90\%$) compared to its nominal value. Similarly, the float mounted on the vehicle (cf. Figure 5) modifies the vector $\boldsymbol{g}^{\star}_{\boldsymbol{\eta}}(\cdot)$ to $\boldsymbol{g}^{\star}_{\boldsymbol{\eta}}(\cdot)+\Delta\boldsymbol{g}^{\star}_{\boldsymbol{\eta}}(\cdot)$ (with $\Delta\boldsymbol{g}^{\star}_{\boldsymbol{\eta}}(\cdot) = +50\%$ w.r.t its nominal value).

To this end, the vehicle tracks the same predefined trajectories designed as in the nominal case. The introduced uncertainties expose the weakness of the PID/PD based schemes, especially in terms of depth tracking, as depicted in Fig. 8 (top left plot). This observation can be easily supported from Fig. 8 (middle left plot). Also, this experiment reveals that the tracking precision of the **MBRISE** controller is less affected despite the parametric uncertainties in the dynamics of the vehicle. Moreover, coupling an HGO or adaptive mechanism or both to the robust control scheme enhances the depth tracking of the UUVs. However, the controller may be much more sensitive to parametric variation such as tether drags. This problem (explicitly pronounced in **OBS-AGSTC**) can slightly degrade the other DOFs trackings, such as the yaw tracking performance in our case, as observed in Fig. 8 (middle right plot). The main reason is that the observer/adaptation dynamics need to be faster than the vehicle's dynamics, which may trigger peaking phenomena for the HGO or high oscillations in the adaptation behavior. Note that the accuracy of the yaw tracking of both the **OBS-GSTC** and the **OBS-AGSTC** can satisfy many control objectives in real-time marine applications, confirmed by the RMS error summarized in Table 3.

Furthermore, we can also notice that the **MBRISE** consumes far less energy compared to all the representative controllers for depth tracking, as shown in Fig. 10. Additionally, this controller is among the representative control schemes with less energy consumption for the yaw tracking task. For easy comparison, we summarize the numerical results of the INT index in Table 4.

3.9.3. *Obtained Results of Scenario 3 (External Disturbances Rejection)*

Recall that this real-time scenario is used to demonstrate a practical marine task, where a robotic arm is installed on the vehicle for the transportation and manipulation of objects (tools, samples, etc.). Based on this notion, we tie a load at the base of the vehicle with an inextensible thread (of negligible mass), as demonstrated in Fig. 6. The main objective is that the vehicle will be abruptly disturbed as it reaches the desired depth of 0.3 m since the load will be resting on the testing pool's floor; hence, this will lead to the cancelling out of the load's effect on the vehicle. The influence of the load is reactivated again when the vehicle is moving vertically upwards to the new desired depth of 0.2 m. Overall, this method produces approximately a similar behaviour representing a sudden dropping or lifting of an object by the vehicle in an underwater site.

The trackings of all the representative control schemes are depicted in Fig. 9 (top plots). From the same figure, we can observe that the attached load prevents the **MBPID** to converge to the desired depth until its influence is deactivated. A static offset reappears on the depth tracking of this controller when the effect of the load becomes active again. In contrast, the remaining controllers neutralize the influence of the load and converge to the desired depth. However, it takes **MBRISE** around 7 seconds to be closed to the desired depth due to the fixed feedback gains of the controller, as shown in Fig. 9 (middle left plot). The yaw trackings, and their tracking error for all the controllers, are shown in Fig. 9 (top and middle right plots, respectively). Moreover, the 3D graphical representation of the depth and the yaw RMSE indices is displayed in Fig. 10. The numerical values of these indices are summarized in Table 3. Note that the aggressive behaviour of the **GSTC** and the observation error of HGO make the yaw trackings of both the **OBS-GSTC** and the **OBS-AGSTC** too sensitive to the vehicle's tether drag. Even though the vehicle receives power as well as the autonomous control signals from the surface station through this tether, it is worth mentioning that it is difficult to manage during the real-time test. The obtained results in Table 4 show approximately less energy consumption in this scenario by all the controllers compared to the previous scenarios; this

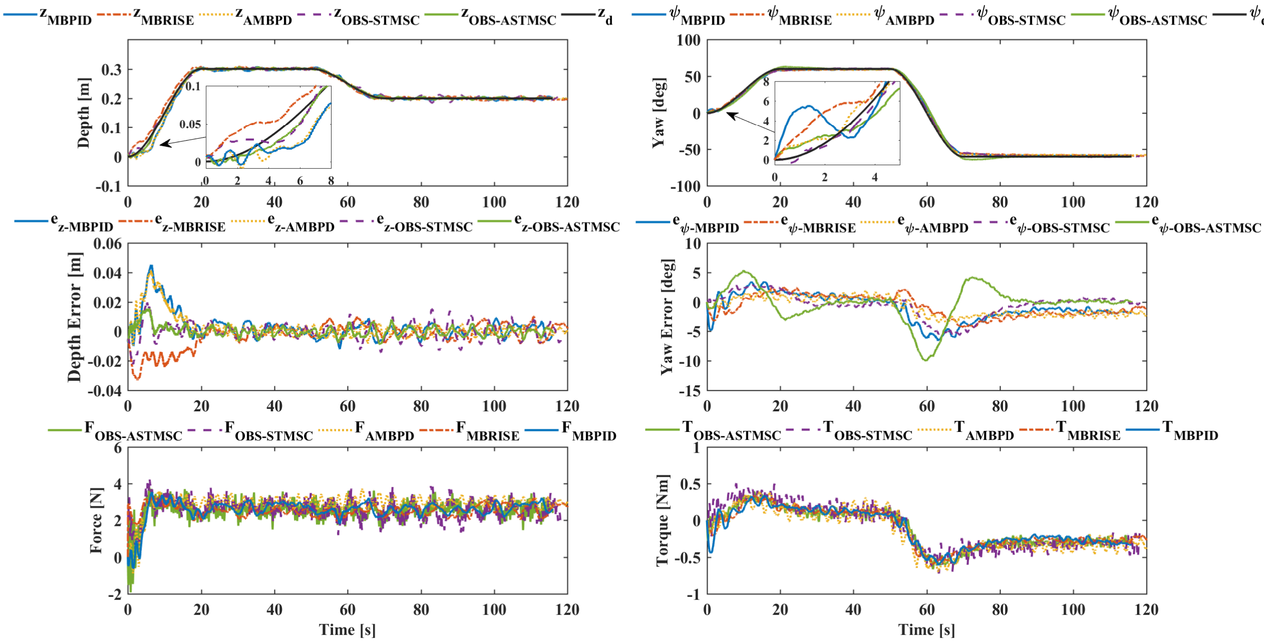

Figure 7: Tracking performance comparison of all the key representative controllers in nominal case: the top plots display the depth and yaw tracking, while their corresponding tracking errors are shown in the middle plots. The bottom plots depict the evolution of the control input signals versus time.

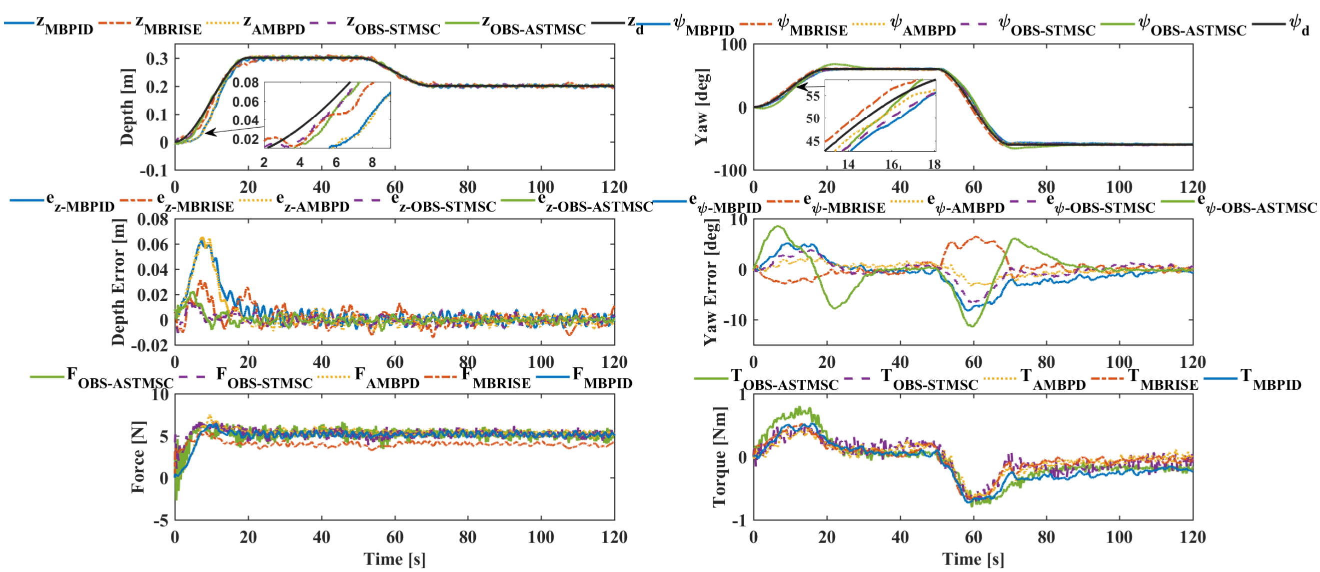

Figure 8: Comparison of the robustness of all the key representative controllers towards parametric uncertainties: the reconfiguration of the vehicle's physical structure changed the matrix $\boldsymbol{D}_{\boldsymbol{\eta}}^{\star}(\cdot)$ and the vector $\boldsymbol{g}_{\boldsymbol{\eta}}^{\star}(\cdot)$ of the vehicle's dynamics to $\boldsymbol{D}_{\boldsymbol{\eta}}^{\star}(\cdot) + \Delta\boldsymbol{D}_{\boldsymbol{\eta}}^{\star}(\cdot)(= +90\%)$ and $\boldsymbol{g}_{\boldsymbol{\eta}}^{\star}(\cdot) + \Delta\boldsymbol{g}_{\boldsymbol{\eta}}^{\star}(\cdot)(= +50\%)$, respectively. The top plots show the depth and yaw trackings, while the tracking errors and the evolution of the control inputs versus time are displayed in the middle and the bottom plots, respectively.

may be due to the load helping to push the vehicle downwards, leading to much less stress on the vehicle's propulsion system. Furthermore, the evolution of the control inputs signals versus time for the depth and the yaw during this mission is depicted in Fig. 9 (bottom plots). Furthermore, the evolution of the control input signals versus time for all the representative controllers during the depth and yaw trackings mission is depicted in Fig. 9 (bottom plots).

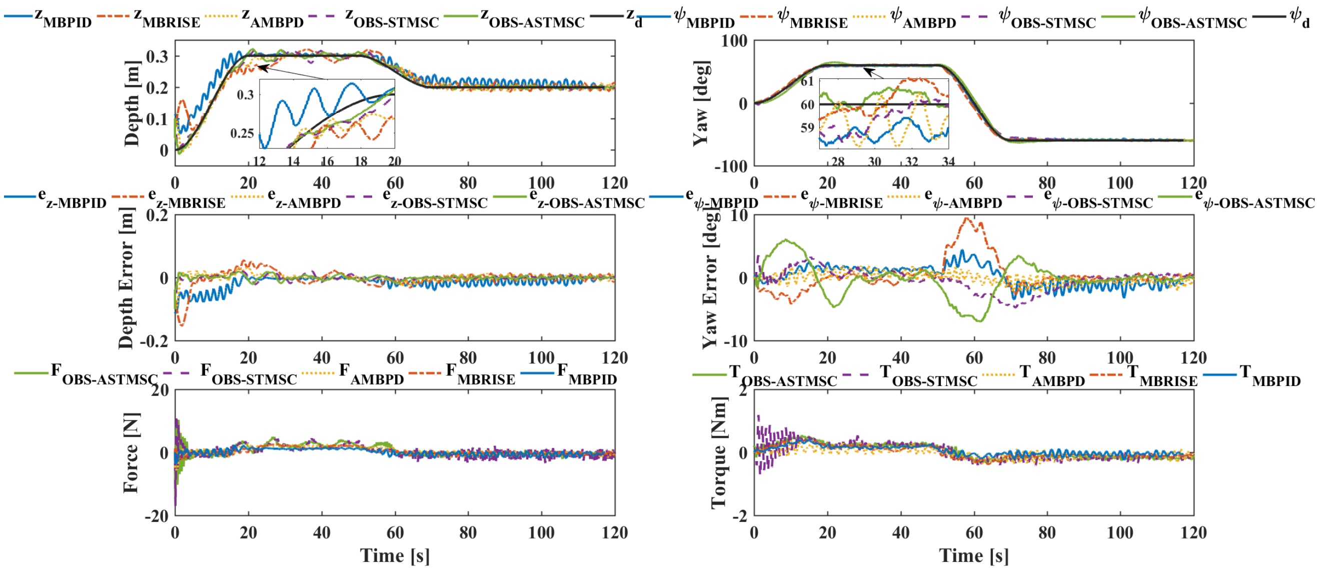

Figure 9: Robustness of all the key representative control schemes towards external disturbances: dropping and lifting of a load.

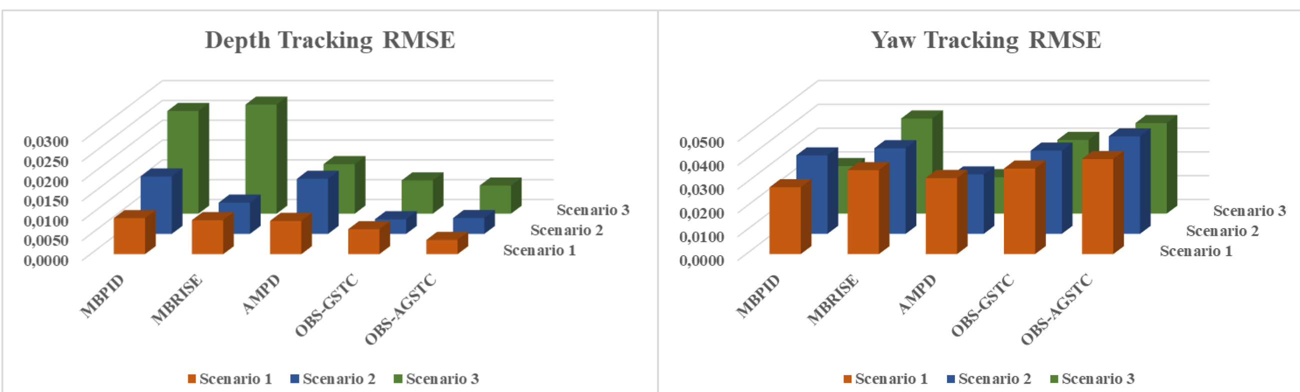

Figure 10: 3D clustered column chart displaying a graphical comparison of depth and yaw RMSE tracking indices for all the representative control schemes.

Table 3
Tracking Performance Based on RMSE Index

Index	Controllers	Scenario 1	Scenario 2	Scenario 3
$RMSE_{depth}$ [$\times10^{-2}$ m]	MBPID	0.91	1.45	2.57
	MBRISE	0.86	0.79	2.75
	AMPD	0.84	1.39	1.25
	OBS-GSTC	0.63	0.37	0.84
	OBS-AGSTC	0.36	0.40	0.71
$RMSE_{yaw}$ [$\times10^{-2}$ deg]	MBPID	2.81	3.30	2.00
	MBRISE	3.53	3.60	4.00
	AMPD	3.20	2.50	1.53
	OBS-GSTC	3.60	3.50	3.10
	OBS-AGSTC	4.00	4.10	3.81

Table 4
Integral of Control Inputs for all the Controllers

Index	Controllers	Scenario 1	Scenario 2	Scenario 3
INT_{depth} [$\times10^{2}$]	MBPID	2.99	6.26	0.97
	MBRISE	2.92	5.02	0.98
	AMPD	3.38	6.54	1.35
	OBS-GSTC	3.04	6.53	1.63
	OBS-AGSTC	2.98	6.39	1.57
INT_{yaw} [$\times10^{2}$]	MBPID	0.28	0.34	0.14
	MBRISE	0.28	0.22	0.19
	AMPD	0.31	0.21	0.15
	OBS-GSTC	0.33	0.26	0.27
	OBS-AGSTC	0.29	0.34	0.24

4. Challenges, Some Potential Investigation Gaps, and Future Trends

Even though many control schemes are proposed for UUVs in the literature, the design and the implementation of autonomous control algorithms on such vehicles for real-time marine tasks still remain an open problem due to several factors like internal perturbations, time-varying external disturbances, UUVs' inherent parametric uncertainties, unmodelled dynamics, unpredictable nature of underwater, etc. This issue becomes much more complex for the case of a fleet of low-cost UUVs. The main reasons include:

- The vehicles are only equipped with a few inexpensive sensors and actuators (e.g. *Leonard UUV*).
- Besides the complex architecture of the majority of the proposed control schemes, exploiting new robotic tools such as the well-known Robot Operating System (ROS) is challenging for real-time applications. Since the nodes of the ROS often communicate via wireless medium to simplify the implementation of these complex autonomous algorithms. In fact, radio communications are almost impossible in underwater environments Awan et al. (2019). An example of an offline application of the ROS on the UUVs can be found in Sukvichai et al. (2016).

According to some selected criteria such as the implementation simplicity, the tracking precision, the low computational cost, the fault-tolerant functionality, and the real-time prospect, most of the research works revisited, in this survey, have less impact on the domain of marine robotics. This proves that there are still more vague investigations gaps, especially when considering real-life applications. Hence, an extra research effort is highly recommended to develop a fully autonomous control scheme for UUVs operating in different underwater environmental settings. The potential control scheme should be able to (i) fulfil the real-time control objectives of different kinds of marine missions; and (ii) adapt intelligently to the dynamic, uncertain, and hostile nature of underwater environments without any modification in its structure. Moreover, this future candidate control scheme should also be able to overcome all the issues faced in day-to-day marine operations using UUVs, as pointed out previously in this work. The future trends may include the following:

1. *Combined control schemes:* It is difficult to design a single autonomous control algorithm satisfying even the most basic marine control objectives due to the well-known issues of both the UUVs and their operating environments. Based on this philosophy, a careful combination of two or more control schemes can be considered a promising direction to deal with some of the problems faced for controlling UUVs.
2. *Communication:* Several intervention operations in marine environments may require the cooperation of multi-agent UUVs. Hence, the simple method to create the desired formation of the vehicle for accomplishing some underwater missions is through robust communication networks. Therefore, distributed control between the multi-agent UUVs can also be considered a domain where more research inputs are needed; this will help in expanding the pipelining technology to the case of complex marine operations.
3. *Observation based control:* Another possibility is deploying the observation-based control scheme to hybrid multi-agent vehicles (operating in the water and the air) for addressing problems like maritime borders surveillance, underwater search and rescue operations, oceanography, deep-sea mining works, divers tracking systems, autonomous disaster management systems, etc.
4. *Other sensitive areas:* They may include fault-tolerant control (FTC). To deploy this technology on UUVs, many technical questions need to be answered, such as how to detect the fault and its severity level as well as its estimate. Then, how to compensate for this fault while the vehicles are still conducting their mission without an interruption Kamel et al. (2020).

5. Conclusion

In this paper, we aim to survey the state of the art of various control schemes developed for the autonomous navigation of unmanned underwater vehicles (UUVs) as well as their design techniques. A simple classification has been proposed to show clearly the advantages and limitations of the main existing control schemes for the UUVs from the literature. Furthermore, a comparative study using representative controllers from the classes has been conducted to investigate the potentials of the schemes for real-life marine operations. To further facilitate the research inputs in the domain of autonomous control of UUVs, critical issues and future trends have been discussed briefly. In the near future, we may consider a similar survey focusing in-depth on all the strategies of model predictive control (MPC) implemented on the UUVs for real-time marine applications. Another recent area we want to investigate thoroughly, as part of our future works, is tracking control issues of the multi-UUV cooperation.

Acknowledgement

The authors acknowledged the Petroleum Technology Development Fund (PTDF), Nigeria, for the first author PhD financial support.

References

Abbasi, A., MahmoudZadeh, S., Yazdani, A., 2022. A cooperative dynamic task assignment framework for cotsbot auvs. IEEE Transactions on Automation Science and Engineering 19, 1163–1179. doi:10.1109/TASE.2020.3044155.

Ahmad, F.F., Ghenai, C., Hamid, A.K., Bettayeb, M., 2020. Application of sliding mode control for maximum power point tracking of solar photovoltaic systems: A comprehensive review. Annual Reviews in Control 49, 173–196.

Ahn, S.S., Ruzzene, M., Scorcelletti, F., Bottasso, C.L., 2010. Configuration optimization of supercavitating underwater vehicles with maneuvering constraints. IEEE Journal of Oceanic Engineering 35, 647–662. doi:10.1109/JOE.2010.2043576.

Ajwad, S.A., Menard, T., Moulay, E., Defoort, M., Coirault, P., 2019. Observer based leader-following consensus of second-order multi-agent systems with nonuniform sampled position data. Journal of the Franklin Institute 356, 10031–10057.

Alessandri, A., Boem, F., 2020. State observers for systems subject to bounded disturbances using quadratic boundedness. IEEE Transactions on Automatic Control 65, 5352–5359. doi:10.1109/TAC.2020.2966720.

Ali, N., Tawiah, I., Zhang, W., 2020. Finite-time extended state observer based nonsingular fast terminal sliding mode control of autonomous underwater vehicles. Ocean Engineering 218, 108179.

Annaswamy, A.M., Fradkov, A.L., 2021. A historical perspective of adaptive control and learning. Annual Reviews in Control .

Antonelli, G., 2003. A new adaptive control law for the phantom rov. IFAC Proceedings Volumes 36, 479–484.

Antonelli, G., 2014. Underwater robots. volume 3. Springer.

Antonelli, G., Caccavale, F., Chiaverini, S., Fusco, G., 2003. A novel adaptive control law for underwater vehicles. IEEE Transactions on Control Systems Technology 11, 221–232. doi:10.1109/TCST.2003.809244.

Antonelli, G., Chiaverini, S., Sarkar, N., West, M., 2001. Adaptive control of an autonomous underwater vehicle: experimental results on odin. IEEE Transactions on Control Systems Technology 9, 756–765. doi:10.1109/87.944470.

Antonelli, G., Fossen, T.I., Yoerger, D.R., 2008. Underwater robotics. Springer handbook of robotics , 987–1008.

Antsaklis, P., 2020. Autonomy and metrics of autonomy. Annual Reviews in Control 49, 15–26.

Atassi, A., Khalil, H., 2000. Separation results for the stabilization of nonlinear systems using different high-gain observer designs. Systems & Control Letters 39, 183–191.

Avila, J.P., Donha, D.C., Adamowski, J.C., 2013. Experimental model identification of open-frame underwater vehicles. Ocean Engineering 60, 81–94.

Awan, K.M., Shah, P.A., Iqbal, K., Gillani, S., Ahmad, W., Nam, Y., 2019. Underwater wireless sensor networks: A review of recent issues and challenges. Wireless Communications and Mobile Computing 2019.

Baruch, A., Mazal, Y., Braginsky, B., Guterman, H., 2020. Attitude estimation of auvs based on a network of pressure sensors. IEEE Sensors Journal 20, 7988–7996. doi:10.1109/JSEN.2020.2982607.

Batmani, Y., Najafi, S., 2019. Event-triggered h^{∞} depth control of remotely operated underwater vehicles. IEEE Transactions on Systems, Man, and Cybernetics: Systems .

Batmani, Y., Najafi, S., 2021. Event-triggered h_{∞} depth control of remotely operated underwater vehicles. IEEE Transactions on Systems, Man, and Cybernetics: Systems 51, 1224–1232. doi:10.1109/TSMC.2019.2896382.

Bejarbaneh, E.Y., Masoumnezhad, M., Armaghani, D.J., Pham, B.T., 2020. Design of robust control based on linear matrix inequality and a novel hybrid pso search technique for autonomous underwater vehicle. Applied Ocean Research 101, 102231.

Bhattacharyya, S., 2017. Robust control under parametric uncertainty: An overview and recent results. Annual Reviews in Control 44, 45–77.

Bi, A., Feng, Z., 2019. Composite hovering control of underwater vehicles via variable ballast systems. Journal of Marine Science and Technology , 1–8.

Bibuli, M., Zereik, E., 2018. Introduction to the special section on marine and maritime robotics: innovation and challenges.

Boehm, J., Berkenpas, E., Shepard, C., Paley, D.A., 2021. Tracking performance of model-based thruster control of a remotely operated underwater vehicle. IEEE Journal of Oceanic Engineering 46, 389–401. doi:10.1109/JOE.2020.2986593.

Borlaug, I.L.G., Pettersen, K.Y., Gravdahl, J.T., 2021. Comparison of two second-order sliding mode control algorithms for an articulated intervention auv: Theory and experimental results. Ocean Engineering 222, 108480.

Borlaug, I.L.G., Pettersen, K.Y., Gravdahl, J.T., 2021. Tracking control of an articulated intervention autonomous underwater vehicle in 6dof using generalized super-twisting: Theory and experiments. IEEE Transactions on Control Systems Technology 29, 353–369. doi:10.1109/TCST.2020.2977302.

Caharija, W., Pettersen, K.Y., Bibuli, M., Calado, P., Zereik, E., Braga, J., Gravdahl, J.T., SÃÿrensen, A.J., MilovanoviÄĞ, M., Bruzzone, G., 2016. Integral line-of-sight guidance and control of underactuated marine vehicles: Theory, simulations, and experiments. IEEE Transactions on Control Systems Technology 24, 1623–1642. doi:10.1109/TCST.2015.2504838.

Campos, E., Chemori, A., Creuze, V., Torres, J., Lozano, R., 2017. Saturation based nonlinear depth and yaw control of underwater vehicles with stability analysis and real-time experiments. Mechatronics 45, 49–59.

Campos, E., Monroy, J., Abundis, H., Chemori, A., Creuze, V., Torres, J., 2019. A nonlinear controller based on saturation functions with variable parameters to stabilize an auv. International Journal of Naval Architecture and Ocean Engineering 11, 211–224.

Chen, Q., Chen, T., Zhang, Y., 2009. Research of ga-based pid for auv motion control, in: 2009 International Conference on Mechatronics and Automation, IEEE. pp. 4446–4451.

Chen, Y., Liu, H., Zhang, Z., Hou, J., Gong, Y., 2018. Nonlinear dynamics modeling and analysis of underwater mud-penetrator steering system. IEEE Access 6, 51206–51216. doi:10.1109/ACCESS.2018.2869386.

Chen, Z., 2019. Nussbaum functions in adaptive control with time-varying unknown control coefficients. Automatica 102, 72–79.

Chu, Z., Wang, D., Meng, F., 2021. An adaptive rbf-nmpc architecture for trajectory tracking control of underwater vehicles. Machines 9, 105.

Cui, J., Zhao, L., Yu, J., Lin, C., Ma, Y., 2019. Neural network-based adaptive finite-time consensus tracking control for multiple autonomous underwater vehicles. IEEE Access 7, 33064–33074.

Cui, R., Chen, L., Yang, C., Chen, M., 2017. Extended state observer-based integral sliding mode control for an underwater robot with unknown disturbances and uncertain nonlinearities. IEEE Transactions on Industrial Electronics 64, 6785–6795. doi:10.1109/TIE.2017.2694410.

Cui, R., Zhang, X., Cui, D., 2016. Adaptive sliding-mode attitude control for autonomous underwater vehicles with input nonlinearities. Ocean Engineering 123, 45–54.

Dabroom, A., Khalil, H., 2001. Output feedback sampled-data control of nonlinear systems using high-gain observers. IEEE Transactions on Automatic Control 46, 1712–1725. doi:10.1109/9.964682.

de CossÃŋo, F.G., Nadri, M., Dufour, P., 2020. Observer design for nonlinear systems with output transformation. IEEE Transactions on Automatic Control 65, 5205–5219. doi:10.1109/TAC.2020.2971934.

Duan, K., Fong, S., Chen, C.P., 2020. Fuzzy observer-based tracking control of an underactuated underwater vehicle with linear velocity estimation. IET Control Theory & Applications 14, 584–593.

Elmokadem, T., Zribi, M., Youcef-Toumi, K., 2017. Terminal sliding mode control for the trajectory tracking of underactuated autonomous underwater vehicles. Ocean Engineering 129, 613–625.

Esfandiari, F., Khalil, H.K., 1992. Output feedback stabilization of fully linearizable systems. International Journal of control 56, 1007–1037.

Eski, İ., Yildirim, S., 2014. Design of neural network control system for controlling trajectory of autonomous underwater vehicles. International Journal of Advanced Robotic Systems 11, 7.

Fischer, N., Hughes, D., Walters, P., Schwartz, E.M., Dixon, W.E., 2014a. Nonlinear rise-based control of an autonomous underwater vehicle. IEEE Transactions on Robotics 30, 845–852. doi:10.1109/TRO.2014.2305791.

Fischer, N., Hughes, D., Walters, P., Schwartz, E.M., Dixon, W.E., 2014b. Nonlinear rise-based control of an autonomous underwater vehicle. IEEE Transactions on Robotics 30, 845–852.

Fossen, T.I., 1999. Guidance and control of ocean vehicles. University of Trondheim, Norway, Printed by John Wiley & Sons, Chichester, England, ISBN: 0 471 94113 1, Doctors Thesis .

Fossen, T.I., 2002. Marine control systems–guidance. navigation, and control of ships, rigs and underwater vehicles. Marine Cybernetics, Trondheim, Norway, Org. Number NO 985 195 005 MVA, www. marinecybernetics. com, ISBN: 82 92356 00 2 .

Gambhire, S., Kishore, D.R., Londhe, P., Pawar, S., 2021. Review of sliding mode based control techniques for control system applications. International Journal of Dynamics and Control 9, 363–378.

Gan, W., Zhu, D., Hu, Z., Shi, X., Yang, L., Chen, Y., 2020. Model predictive adaptive constraint tracking control for underwater vehicles. IEEE Transactions on Industrial Electronics 67, 7829–7840. doi:10.1109/TIE.2019.2941132.

Gan, W., Zhu, D., Ji, D., 2018. Qpso-model predictive control-based approach to dynamic trajectory tracking control for unmanned underwater vehicles. Ocean Engineering 158, 208–220.

Gan, W.Y., Zhu, D.Q., Xu, W.L., Sun, B., 2017. Survey of trajectory tracking control of autonomous underwater vehicles. Journal of marine science and technology 25, 13.

Gao, Z., Guo, G., 2019. Velocity free leader-follower formation control for autonomous underwater vehicles with line-of-sight range and angle constraints. Information Sciences 486, 359–378.

García-Valdovinos, L.G., Fonseca-Navarro, F., Aizpuru-Zinkunegi, J., Salgado-Jiménez, T., Gómez-Espinosa, A., Cruz-Ledesma, J.A., 2019. Neuro-sliding control for underwater rovâĂŹs subject to unknown disturbances. Sensors 19, 2943.

Garcia-Valdovinos, L.G., Salgado-Jimenez, T., 2011. On the dynamic positioning control of underwater vehicles subject to ocean currents, in: 2011 8th International Conference on Electrical Engineering, Computing Science and Automatic Control, pp. 1–6. doi:10.1109/ICEEE.2011.6106590.

Garcia-Valdovinos, L.G., Salgado-JimÃĺnez, T., Torres-RodrÃŋguez, H., 2009. Model-free high order sliding mode control for rov: Station-keeping approach, in: OCEANS 2009, pp. 1–7. doi:10.23919/OCEANS.2009.5422455.

Geder, J.D., Palmisano, J., Ramamurti, R., Sandberg, W.C., Ratna, B., 2008. Fuzzy logic pid based control design and performance for a pectoral fin propelled unmanned underwater vehicle, in: 2008 International Conference on Control, Automation and Systems, IEEE. pp. 40–46.

Gibson, S.B., Stilwell, D.J., 2020. Hydrodynamic parameter estimation for autonomous underwater vehicles. IEEE Journal of Oceanic Engineering 45, 385–394. doi:10.1109/JOE.2018.2877489.

González-García, J., Narcizo-Nuci, N.A., García-Valdovinos, L.G., Salgado-Jiménez, T., Gómez-Espinosa, A., Cuan-Urquizo, E., Cabello, J.A.E., 2021. Model-free high order sliding mode control with finite-time tracking for unmanned underwater vehicles. Applied Sciences 11, 1836.

Guerrero, J., Torres, J., Creuze, V., Chemori, A., 2019a. Observation-based nonlinear proportional–derivative control for robust trajectory tracking for autonomous underwater vehicles. IEEE Journal of Oceanic Engineering .

Guerrero, J., Torres, J., Creuze, V., Chemori, A., 2019b. Trajectory tracking for autonomous underwater vehicle: An adaptive approach. Ocean Engineering 172, 511–522.

Guerrero, J., Torres, J., Creuze, V., Chemori, A., 2020a. Adaptive disturbance observer for trajectory tracking control of underwater vehicles. Ocean Engineering 200, 107080.

Guerrero, J., Torres, J., Creuze, V., Chemori, A., 2020b. Observation-based nonlinear proportionalâĂŞderivative control for robust trajectory tracking for autonomous underwater vehicles. IEEE Journal of Oceanic Engineering 45, 1190–1202. doi:10.1109/JOE.2019.2924561.

Guerrero, J., Torres, J., Creuze, V., Chemori, A., Campos, E., 2019c. Saturation based nonlinear pid control for underwater vehicles: Design, stability analysis and experiments. Mechatronics 61, 96–105.

Han, G., Gong, A., Wang, H., MartÃŋnez-GarcÃŋa, M., Peng, Y., 2021. Multi-auv collaborative data collection algorithm based on q-learning in underwater acoustic sensor networks. IEEE Transactions on Vehicular Technology 70, 9294–9305. doi:10.1109/TVT.2021.3097084.

Hao, L.Y., Zhang, H., Guo, G., Li, H., 2019. Quantized sliding mode control of unmanned marine vehicles: Various thruster faults tolerated with a unified model. IEEE Transactions on Systems, Man, and Cybernetics: Systems .

Harris, Z.J., Whitcomb, L.L., 2021. Cooperative acoustic navigation of underwater vehicles without a dvl utilizing a dynamic process model: Theory and field evaluation. Journal of Field Robotics .

Hassanein, O., Anavatti, S.G., Shim, H., Ray, T., 2016. Model-based adaptive control system for autonomous underwater vehicles. Ocean Engineering 127, 58–69.

Hernández-Alvarado, R., García-Valdovinos, L.G., Salgado-Jiménez, T., Gómez-Espinosa, A., Fonseca-Navarro, F., 2016. Neural network-based self-tuning pid control for underwater vehicles. Sensors 16, 1429.

Heshmati-alamdari, S., Nikou, A., Dimarogonas, D.V., 2019. Robust trajectory tracking control for underactuated autonomous underwater vehicles, in: 2019 IEEE 58th Conference on Decision and Control (CDC), pp. 8311–8316. doi:10.1109/CDC40024.2019.9030165.

Heshmati-Alamdari, S., Nikou, A., Dimarogonas, D.V., 2021. Robust trajectory tracking control for underactuated autonomous underwater vehicles in uncertain environments. IEEE Transactions on Automation Science and Engineering 18, 1288–1301. doi:10.1109/TASE.2020.3001183.

Hou, S.P., Cheah, C.C., 2009. Pd control scheme for formation control of multiple autonomous underwater vehicles, in: 2009 IEEE/ASME International Conference on Advanced Intelligent Mechatronics, pp. 356–361. doi:10.1109/AIM.2009.5229987.

Hou, S.P., Cheah, C.C., 2011. Can a simple control scheme work for a formation control of multiple autonomous underwater vehicles? IEEE Transactions on Control Systems Technology 19, 1090–1101. doi:10.1109/TCST.2010.2076388.

Hu, B., Tian, H., Qian, J., Xie, G., Mo, L., Zhang, S., 2013. A fuzzy-pid method to improve the depth control of auv, in: 2013 IEEE International Conference on Mechatronics and Automation, IEEE. pp. 1528–1533.

Hu, K., Chen, X., Weng, L., Tian, L., Hu, Y., 2020. A survey of deep neural network sliding mode control in robot application, in: 2020 Chinese Automation Congress (CAC), IEEE. pp. 6659–6662.

Ippoliti, G., Jetto, L., Longhi, S., 2005. Improved set-points tracking of remotely operated underwater vehicles through a supervised pid control scheme. Journal of Marine Engineering & Technology 4, 3–9.

Izadbakhsh, A., Khorashadizadeh, S., Kheirkhahan, P., 2019. Tracking control of electrically driven robots using a model-free observer. Robotica 37, 729–755.

Jaffe, J.S., Franks, P.J., Roberts, P.L., Mirza, D., Schurgers, C., Kastner, R., Boch, A., 2017. A swarm of autonomous miniature underwater robot drifters for exploring submesoscale ocean dynamics. Nature communications 8, 1–8.

Ji, D., Yao, X., Li, S., Tang, Y., Tian, Y., 2021. Model-free fault diagnosis for autonomous underwater vehicles using sequence convolutional neural network. Ocean Engineering 232, 108874.

Jia, Z., Qiao, L., Zhang, W., 2020. Adaptive tracking control of unmanned underwater vehicles with compensation for external perturbations and uncertainties using port-hamiltonian theory. Ocean Engineering 209, 107402.

Jiang, P., Song, S., Huang, G., 2021. Attention-based meta-reinforcement learning for tracking control of auv with time-varying dynamics. IEEE Transactions on Neural Networks and Learning Systems , 1–14doi:10.1109/TNNLS.2021.3079148.

Jin, S., Bak, J., Kim, J., Seo, T., Kim, H.S., 2018. Switching pd-based sliding mode control for hovering of a tilting-thruster underwater robot. Plos one 13, e0194427.

Kamel, M.A., Yu, X., Zhang, Y., 2020. Formation control and coordination of multiple unmanned ground vehicles in normal and faulty situations: A review. Annual reviews in control 49, 128–144.

Karimi, H.R., Lu, Y., 2021. Guidance and control methodologies for marine vehicles: A survey. Control Engineering Practice 111, 104785.

Karras, G.C., Bechlioulis, C.P., Nagappa, S., Palomeras, N., Kyriakopoulos, K.J., Carreras, M., 2014. Motion control for autonomous underwater vehicles: A robust model âĂŤ free approach, in: 2014 IEEE International Conference on Robotics and Automation (ICRA), pp. 6529–6534. doi:10.1109/ICRA.2014.6907822.

Kelly, R., Davila, V.S., Perez, J.A.L., 2006. Control of robot manipulators in joint space. Springer Science & Business Media.

Khalid, M.U., Ahsan, M., Kamal, O., Najeeb, U., 2019. Modeling and trajectory tracking of remotely operated underwater vehicle using higher order sliding mode control, in: 2019 16th International Bhurban Conference on Applied Sciences and Technology (IBCAST), pp. 855–860. doi:10.1109/IBCAST.2019.8667200.

Khalil, H.K., 2008. High-gain observers in nonlinear feedback control, in: 2008 International Conference on Control, Automation and Systems, pp. xlvii–lvii. doi:10.1109/ICCAS.2008.4694705.

Khalil, H.K., Praly, L., 2014. High-gain observers in nonlinear feedback control. International Journal of Robust and Nonlinear Control 24, 993–1015.

Khodayari, M.H., Balochian, S., 2015. Modeling and control of autonomous underwater vehicle (auv) in heading and depth attitude via self-adaptive fuzzy pid controller. Journal of Marine Science and Technology 20, 559–578.

Kim, D.W., 2015. Tracking of remus autonomous underwater vehicles with actuator saturations. Automatica (Journal of IFAC) 58, 15–21.

Kim, M., Joe, H., Pyo, J., Kim, J., Kim, H., Yu, S.c., 2013. Variable-structure pid controller with anti-windup for autonomous underwater vehicle, in: 2013 OCEANS-San Diego, IEEE. pp. 1–5.

Kong, S., Sun, J., Qiu, C., Wu, Z., Yu, J., 2021. Extended state observer-based controller with model predictive governor for 3-d trajectory tracking of underactuated underwater vehicles. IEEE Transactions on Industrial Informatics 17, 6114–6124. doi:10.1109/TII.2020.3036665.

Kumar, M., Mondal, S., 2021. Recent developments on target tracking problems: A review. Ocean Engineering 236, 109558.

Kumar, N., Rani, M., 2020. An efficient hybrid approach for trajectory tracking control of autonomous underwater vehicles. Applied Ocean Research 95, 102053.

Kumar, R.P., Dasgupta, A., Kumar, C., 2007. Robust trajectory control of underwater vehicles using time delay control law. Ocean Engineering 34, 842–849.

Li, H., Xie, P., Yan, W., 2017. Receding horizon formation tracking control of constrained underactuated autonomous underwater vehicles. IEEE Transactions on Industrial Electronics 64, 5004–5013. doi:10.1109/TIE.2016.2589921.

Li, M., Guo, C., Yu, H., Yuan, Y., 2021. Line-of-sight-based global finite-time stable path following control of unmanned surface vehicles with actuator saturation. ISA transactions .

Li, S., Wang, X., Zhang, L., 2015. Finite-time output feedback tracking control for autonomous underwater vehicles. IEEE Journal of Oceanic Engineering 40, 727–751. doi:10.1109/JOE.2014.2330958.

Li, X., Ren, C., Ma, S., Zhu, X., 2020. Compensated model-free adaptive tracking control scheme for autonomous underwater vehicles via extended state observer. Ocean Engineering 217, 107976.

Li, Y., Li, B., Yu, W., Zhu, S., Guan, X., 2022. Cooperative localization based multi-auv trajectory planning for target approaching in anchor-free environments. IEEE Transactions on Vehicular Technology 71, 3092–3107. doi:10.1109/TVT.2021.3137171.

Lin, C., Feng, X., Gong, P., Jin, Z., 2008. An application of the improved hybrid fuzzy pid control system, in: 2008 7th World Congress on Intelligent Control and Automation, IEEE. pp. 5704–5709.

Lin, M., Yang, C., Li, D., 2020. Hybrid strategy based model parameter estimation of irregular-shaped underwater vehicles for predicting velocity. Robotics and Autonomous Systems 127, 103480.

Liu, F., Tang, H., Qin, Y., Duan, C., Luo, J., Pu, H., 2022. Review on fault diagnosis of unmanned underwater vehicles. Ocean Engineering 243, 110290.

Liu, H., Lyu, Y., Lewis, F.L., Wan, Y., 2019a. Robust time-varying formation control for multiple underwater vehicles subject to nonlinearities and uncertainties. International Journal of Robust and Nonlinear Control 29, 2712–2724.

Liu, H., Wang, Y., Lewis, F.L., 2021a. Robust distributed formation controller design for a group of unmanned underwater vehicles. IEEE Transactions on Systems, Man, and Cybernetics: Systems 51, 1215–1223. doi:10.1109/TSMC.2019.2895499.

Liu, L., Zhang, L., Zhang, S., Cao, S., 2020. Multi-uuv cooperative dynamic maneuver decision-making algorithm using intuitionistic fuzzy game theory. Complexity 2020.

Liu, S., Liu, Y., Wang, N., 2017. Nonlinear disturbance observer-based backstepping finite-time sliding mode tracking control of underwater vehicles with system uncertainties and external disturbances. Nonlinear Dynamics 88, 465–476.

Liu, X., Zhang, M., Rogers, E., 2019b. Trajectory tracking control for autonomous underwater vehicles based on fuzzy re-planning of a local desired trajectory. IEEE Transactions on Vehicular Technology 68, 11657–11667. doi:10.1109/TVT.2019.2948153.

Liu, X., Zhang, M., Rogers, E., Wang, Y., Yao, F., 2021b. Terminal sliding mode-based tracking control with error transformation for underwater vehicles. International Journal of Robust and Nonlinear Control .

Liu, X., Zhang, M., Yao, F., Yin, B., Chen, J., 2021c. Barrier lyapunov function based adaptive region tracking control for underwater vehicles with thruster saturation and dead zone. Journal of the Franklin Institute .

Londhe, P.S., Patre, B., Waghmare, L.M., Santhakumar, M., 2017. Robust proportional derivative (pd)-like fuzzy control designs for diving and steering planes control of an autonomous underwater vehicle. Journal of Intelligent & Fuzzy Systems 32, 2509–2522.

Maalouf, D., Chemori, A., Creuze, V., 2013. Stability analysis of a new extended l1 controller with experimental validation on an underwater vehicle, in: 52nd IEEE Conference on Decision and Control, pp. 6149–6155. doi:10.1109/CDC.2013.6760861.

Maalouf, D., Chemori, A., Creuze, V., 2015a. L1 adaptive depth and pitch control of an underwater vehicle with real-time experiments. Ocean Engineering 98, 66–77.

Maalouf, D., Creuze, V., Chemori, A., Tamanaja, I.T., Mercado, E.C., Muñoz, J.T., Lozano, R., Tempier, O., 2015b. Real-time experimental comparison of two depth control schemes for underwater vehicles. International Journal of Advanced Robotic Systems 12, 13.

Makavita, C.D., Jayasinghe, S.G., Nguyen, H.D., Ranmuthugala, D., 2019. Experimental study of command governor adaptive control for unmanned underwater vehicles. IEEE Transactions on Control Systems Technology 27, 332–345. doi:10.1109/TCST.2017.2757021.

Martin, S.C., Whitcomb, L.L., 2012. Preliminary experiments in nonlinear model-based tracking control of underwater vehicles with three degree-of-freedom fully-coupled dynamical plant models, in: 2012 Oceans, pp. 1–9. doi:10.1109/OCEANS.2012.6404841.

Martin, S.C., Whitcomb, L.L., 2013. Preliminary experiments in fully actuated model based control with six degree-of-freedom coupled dynamical plant models for underwater vehicles, in: 2013 IEEE International Conference on Robotics and Automation, pp. 4621–4628. doi:10.1109/ICRA.2013.6631234.

Martin, S.C., Whitcomb, L.L., 2018. Nonlinear model-based tracking control of underwater vehicles with three degree-of-freedom fully coupled dynamical plant models: Theory and experimental evaluation. IEEE Transactions on Control Systems Technology 26, 404–414. doi:10.1109/TCST.2017.2665974.

McMahon, J., Plaku, E., 2016. Mission and motion planning for autonomous underwater vehicles operating in spatially and temporally complex environments. IEEE Journal of Oceanic Engineering 41, 893–912. doi:10.1109/JOE.2015.2503498.

Meurer, C., Fuentes-PÃĩrez, J.F., SchwarzwÃďlder, K., Ludvigsen, M., SÃÿrensen, A.J., Kruusmaa, M., 2020. 2d estimation of velocity relative to water and tidal currents based on differential pressure for autonomous underwater vehicles. IEEE Robotics and Automation Letters 5, 3444–3451. doi:10.1109/LRA.2020.2976318.

Miao, B., Li, T., Luo, W., 2013. A dsc and mlp based robust adaptive nn tracking control for underwater vehicle. Neurocomputing 111, 184–189.

Morato, M.M., Normey-Rico, J.E., Sename, O., 2020. Model predictive control design for linear parameter varying systems: A survey. Annual Reviews in Control 49, 64–80.

Nađ, Đ., Mišković, N., Mandić, F., 2015. Navigation, guidance and control of an overactuated marine surface vehicle. Annual Reviews in Control 40, 172–181.

Neira, J., Sequeiros, C., Huamani, R., Machaca, E., Fonseca, P., Nina, W., 2021. Review on unmanned underwater robotics, structure designs, materials, sensors, actuators, and navigation control. Journal of Robotics 2021.

Noguchi, Y., Maki, T., 2021. Tracking omnidirectional surfaces using a low-cost autonomous underwater vehicle. IEEE Journal of Oceanic Engineering 46, 11–23. doi:10.1109/JOE.2020.2972046.

Pan, H., Xin, M., 2012. Depth control of autonomous underwater vehicles using indirect robust control method. International Journal of Control 85, 98–113.

Peng, Z., Wang, J., Wang, D., Han, Q.L., 2021. An overview of recent advances in coordinated control of multiple autonomous surface vehicles. IEEE Transactions on Industrial Informatics 17, 732–745. doi:10.1109/TII.2020.3004343.

Peng, Z., Wang, J., Wang, J., 2019. Constrained control of autonomous underwater vehicles based on command optimization and disturbance estimation. IEEE Transactions on Industrial Electronics 66, 3627–3635. doi:10.1109/TIE.2018.2856180.

Plamondon, N., Nahon, M., 2008. Trajectory tracking controller for an underwater hexapod vehicle, in: OCEANS 2008, pp. 1–8. doi:10.1109/OCEANS.2008.5151830.

Qiao, L., Zhang, W., 2019. Adaptive second-order fast nonsingular terminal sliding mode tracking control for fully actuated autonomous underwater vehicles. IEEE Journal of Oceanic Engineering 44, 363–385. doi:10.1109/JOE.2018.2809018.

Qiu, J., Ma, M., Wang, T., Gao, H., 2021. Gradient descent-based adaptive learning control for autonomous underwater vehicles with unknown uncertainties. IEEE Transactions on Neural Networks and Learning Systems , 1–8doi:10.1109/TNNLS.2021.3056585.

Ridao, P., Carreras, M., Ribas, D., Sanz, P.J., Oliver, G., 2015. Intervention auvs: the next challenge. Annual Reviews in Control 40, 227–241.

Saback, R.M., Conceicao, A.G.S., Santos, T.L.M., Albiez, J., Reis, M., 2019. Nonlinear model predictive control applied to an autonomous underwater vehicle. IEEE Journal of Oceanic Engineering .

Safaei, A., Mahyuddin, M.N., 2018. Application of the optimal adaptive model-free control algorithm on an autonomous underwater vehicle, in: 2018 3rd International Conference on Advanced Robotics and Mechatronics (ICARM), pp. 346–350. doi:10.1109/ICARM.2018.8610716.

Sahu, B.K., Subudhi, B., 2014. Adaptive tracking control of an autonomous underwater vehicle. International Journal of Automation and Computing 11, 299–307.

Saied, H., Chemori, A., El Rafei, M., Francis, C., Pierrot, F., 2019. From non-model-based to model-based control of pkms: a comparative study, in: Mechanism, Machine, Robotics and Mechatronics Sciences. Springer, pp. 153–169.

Salgado-Jiménez, T., García-Valdovinos, L.G., Delgado-Ramírez, G., Bartoszewicz, A., 2011. Control of rovs using a model-free 2nd-order sliding mode approach. Sliding mode control , 347–368.

Seok Park, B., 2015. Neural network-based tracking control of underactuated autonomous underwater vehicles with model uncertainties. Journal of Dynamic Systems, Measurement, and Control 137.

Shen, C., Shi, Y., Buckham, B., 2018. Trajectory tracking control of an autonomous underwater vehicle using lyapunov-based model predictive control. IEEE Transactions on Industrial Electronics 65, 5796–5805. doi:10.1109/TIE.2017.2779442.

Shi, L., Zheng, R., Zhang, S., Liu, M., 2021. Cooperative estimation to reconstruct the parametric flow field using multiple auvs. IEEE Transactions on Instrumentation and Measurement 70, 1–10. doi:10.1109/TIM.2021.3127634.

Shi, Y., Zhang, K., 2021. Advanced model predictive control framework for autonomous intelligent mechatronic systems: A tutorial overview and perspectives. Annual Reviews in Control 52, 170–196.

Simetti, E., Campos, R., Vito, D.D., Quintana, J., Antonelli, G., Garcia, R., Turetta, A., 2021a. Sea mining exploration with an uvms: Experimental validation of the control and perception framework. IEEE/ASME Transactions on Mechatronics 26, 1635–1645. doi:10.1109/TMECH.2020.3025973.

Simetti, E., Indiveri, G., Pascoal, A.M., 2021b. Wimust: A cooperative marine robotic system for autonomous geotechnical surveys. Journal of Field Robotics 38, 268–288.

Smallwood, D., Whitcomb, L., 2004. Model-based dynamic positioning of underwater robotic vehicles: theory and experiment. IEEE Journal of Oceanic Engineering 29, 169–186. doi:10.1109/JOE.2003.823312.

Somefun, O.A., Akingbade, K., Dahunsi, F., 2021. The dilemma of pid tuning. Annual Reviews in Control 52, 65–74.

Song, Y.S., Arshad, M.R., 2016. Tracking control design for autonomous underwater vehicle using robust filter approach, in: 2016 IEEE/OES Autonomous Underwater Vehicles (AUV), pp. 374–380. doi:10.1109/AUV.2016.7778699.

Soylu, S., Buckham, B.J., Podhorodeski, R.P., 2007. Robust control of underwater vehicles with fault-tolerant infinity-norm thruster force allocation, in: OCEANS 2007, pp. 1–10. doi:10.1109/OCEANS.2007.4449388.

Su, X., Shi, P., Wu, L., Song, Y.D., 2016. Fault detection filtering for nonlinear switched stochastic systems. IEEE Transactions on Automatic Control 61, 1310–1315. doi:10.1109/TAC.2015.2465091.

Sukvichai, K., Wongsuwan, K., Kaewnark, N., Wisanuvej, P., 2016. Implementation of visual odometry estimation for underwater robot on ros by using raspberrypi 2, in: 2016 International Conference on Electronics, Information, and Communications (ICEIC), pp. 1–4. doi:10.1109/ELINFOCOM.2016.7563010.

Sun, S., Song, B., Wang, P., Dong, H., Chen, X., 2022. Real-time mission-motion planner for multi-uuvs cooperative work using tri-level programing. IEEE Transactions on Intelligent Transportation Systems 23, 1260–1273. doi:10.1109/TITS.2020.3023819.

Sun, Y., Cheah, C., 2003. Adaptive setpoint control for autonomous underwater vehicles, in: 42nd IEEE International Conference on Decision and Control (IEEE Cat. No. 03CH37475), IEEE. pp. 1262–1267.

Teeneti, C.R., Truscott, T.T., Beal, D.N., Pantic, Z., 2021. Review of wireless charging systems for autonomous underwater vehicles. IEEE Journal of Oceanic Engineering 46, 68–87. doi:10.1109/JOE.2019.2953015.

Theunissen, J., Tota, A., Gruber, P., Dhaens, M., Sorniotti, A., 2021. Preview-based techniques for vehicle suspension control: a state-of-the-art review. Annual Reviews in Control 51, 206–235.

Tijjani, A.S., Chemori, A., 2020. From Non-Model-Based to Adaptive Model-Based Tracking Control of Low-Inertia Underwater Vehicles, in: Underwater Vehicles: Design and Applications. URL: https://hal-lirmm.ccsd.cnrs.fr/lirmm-03009836.

Tijjani, A.S., Chemori, A., 2021. From Non-Model-Based to Adaptive Model-Based Tracking Control of Low-Inertia Underwater Vehicles. in Underwater Vehicles: Design and Applications, Ed Nova Science Publishers - INC, ISBN: 978-1-53618-876-9.

Tijjani, A.S., Chemori, A., Creuze, V., 2021. Robust adaptive tracking control of underwater vehicles: Design, stability analysis, and experiments. IEEE/ASME Transactions on Mechatronics 26, 897–907. doi:10.1109/TMECH.2020.3012502.

Tumari, M.Z.M., Abidin, A.F.Z., Hussin, M.S.F., Abd Kadir, A.M., Aras, M.S.M., Ahmad, M.A., 2019. Pso fine-tuned model-free pid controller with derivative filter for depth control of hovering autonomous underwater vehicle, in: Proceedings of the 10th National Technical Seminar on Underwater System Technology 2018, Springer. pp. 3–13.

Vu, M.T., Le Thanh, H.N.N., Huynh, T.T., Thang, Q., Duc, T., Hoang, Q.D., Le, T.H., 2021. Station-keeping control of a hovering over-actuated autonomous underwater vehicle under ocean current effects and model uncertainties in horizontal plane. IEEE Access 9, 6855–6867. doi:10.1109/ACCESS.2020.3048706.

Wan, J., He, B., Wang, D., Yan, T., Shen, Y., 2019. Fractional-order pid motion control for auv using cloud-model-based quantum genetic algorithm. IEEE Access 7, 124828–124843. doi:10.1109/ACCESS.2019.2937978.

Wang, B., Mihalec, M., Gong, Y., Pompili, D., Yi, J., 2018a. Disturbance observer-based motion control of small autonomous underwater vehicles, in: Dynamic Systems and Control Conference, American Society of Mechanical Engineers. p. V003T35A004.

Wang, H., Tian, Y., Xu, H., 2022. Neural adaptive command filtered control for cooperative path following of multiple underactuated autonomous underwater vehicles along one path. IEEE Transactions on Systems, Man, and Cybernetics: Systems 52, 2966–2978. doi:10.1109/TSMC.2021.3062077.

Wang, J., Zhou, Z., Wang, C., Ding, Z., 2020a. Cascade structure predictive observer design for consensus control with applications to uavs formation flying. Automatica 121, 109200.

Wang, N., Su, S.F., 2021. Finite-time unknown observer-based interactive trajectory tracking control of asymmetric underactuated surface vehicles. IEEE Transactions on Control Systems Technology 29, 794–803. doi:10.1109/TCST.2019.2955657.

Wang, N., Su, S.F., Yin, J., Zheng, Z., Er, M.J., 2018b. Global asymptotic model-free trajectory-independent tracking control of an uncertain marine vehicle: An adaptive universe-based fuzzy control approach. IEEE Transactions on Fuzzy Systems 26, 1613–1625. doi:10.1109/TFUZZ.2017.2737405.

Wang, W., Xia, Y., Chen, Y., Xu, G., Chen, Z., Xu, K., 2020b. Motion control methods for x-rudder underwater vehicles: Model based sliding mode and non-model based iterative sliding mode. Ocean Engineering 216, 108054.

Wang, Y., Gu, L., Gao, M., Zhu, K., 2016. Multivariable output feedback adaptive terminal sliding mode control for underwater vehicles. Asian Journal of Control 18, 247–265.

Wang, Y., Gu, L., Luo, G., Li, X., Zhou, F., Cao, X., Chen, J., 2015. Depth control of rovs using time delay estimation with nonsingular terminal sliding mode, in: OCEANS 2015 - MTS/IEEE Washington, pp. 1–6. doi:10.23919/OCEANS.2015.7401804.

Wu, J., Song, C., Ma, J., Wu, J., Han, G., 2021. Reinforcement learning and particle swarm optimization supporting real-time rescue assignments for multiple autonomous underwater vehicles. IEEE Transactions on Intelligent Transportation Systems , 1–14doi:10.1109/TITS.2021.3062500.

Wu, Y., Low, K.H., Lv, C., 2020. Cooperative path planning for heterogeneous unmanned vehicles in a search-and-track mission aiming at an underwater target. IEEE Transactions on Vehicular Technology 69, 6782–6787. doi:10.1109/TVT.2020.2991983.

Xian, B., Dawson, D., de Queiroz, M., Chen, J., 2004. A continuous asymptotic tracking control strategy for uncertain nonlinear systems. IEEE Transactions on Automatic Control 49, 1206–1211. doi:10.1109/TAC.2004.831148.

Xiang, X., Yu, C., Lapierre, L., Zhang, J., Zhang, Q., 2018. Survey on fuzzy-logic-based guidance and control of marine surface vehicles and underwater vehicles. International Journal of Fuzzy Systems 20, 572–586.

Xu, B., Li, S., Razzaqi, A.A., Guo, Y., Wang, L., 2021. A novel measurement information anomaly detection method for cooperative localization. IEEE Transactions on Instrumentation and Measurement 70, 1–18. doi:10.1109/TIM.2021.3077981.

Xu, F., Zou, Z.J., Yin, J.C., Cao, J., 2013. Identification modeling of underwater vehicles' nonlinear dynamics based on support vector machines. Ocean Engineering 67, 68–76.

Xu, J., Wang, M., Qiao, L., 2015. Dynamical sliding mode control for the trajectory tracking of underactuated unmanned underwater vehicles. Ocean engineering 105, 54–63.

Yan, J., Gao, J., Yang, X., Luo, X., Guan, X., 2020a. Position tracking control of remotely operated underwater vehicles with communication delay. IEEE Transactions on Control Systems Technology 28, 2506–2514. doi:10.1109/TCST.2019.2928488.

Yan, Y., Yu, S., 2018. Sliding mode tracking control of autonomous underwater vehicles with the effect of quantization. Ocean Engineering 151, 322–328.

Yan, Z., Gong, P., Zhang, W., Wu, W., 2020b. Model predictive control of autonomous underwater vehicles for trajectory tracking with external disturbances. Ocean Engineering 217, 107884.

Yang, X., Yan, J., Hua, C., Guan, X., 2019. Trajectory tracking control of autonomous underwater vehicle with unknown parameters and external disturbances. IEEE Transactions on Systems, Man, and Cybernetics: Systems .

Yang, X., Yan, J., Hua, C., Guan, X., 2021a. Trajectory tracking control of autonomous underwater vehicle with unknown parameters and external disturbances. IEEE Transactions on Systems, Man, and Cybernetics: Systems 51, 1054–1063. doi:10.1109/TSMC.2019.2894171.

Yang, Y., Xiao, Y., Li, T., 2021b. A survey of autonomous underwater vehicle formation: Performance, formation control, and communication capability. IEEE Communications Surveys Tutorials 23, 815–841. doi:10.1109/COMST.2021.3059998.

Yu, C., Xiang, X., Wilson, P.A., Zhang, Q., 2020. Guidance-error-based robust fuzzy adaptive control for bottom following of a flight-style auv with saturated actuator dynamics. IEEE Transactions on Cybernetics 50, 1887–1899. doi:10.1109/TCYB.2018.2890582.

Yuh, J., 2000. Design and control of autonomous underwater robots: A survey. Autonomous Robots 8, 7–24.

Yuh, J., West, M., Lee, P., 2001. An autonomous underwater vehicle control with a non-regressor based algorithm, in: Proceedings 2001 ICRA. IEEE International Conference on Robotics and Automation (Cat. No.01CH37164), pp. 2363–2368 vol.3. doi:10.1109/ROBOT.2001.932975.

Zemouche, A., Zhang, F., Mazenc, F., Rajamani, R., 2019. High-gain nonlinear observer with lower tuning parameter. IEEE Transactions on Automatic Control 64, 3194–3209. doi:10.1109/TAC.2018.2882417.

Zhang, D., Wei, B., 2017. A review on model reference adaptive control of robotic manipulators. Annual Reviews in Control 43, 188–198.

Zhang, J., Han, G., Sha, J., Qian, Y., Liu, J., 2022. Auv-assisted subsea exploration method in 6g enabled deep ocean based on a cooperative pac-men mechanism. IEEE Transactions on Intelligent Transportation Systems 23, 1649–1660. doi:10.1109/TITS.2021.3102995.

Zhang, J., Sha, J., Han, G., Liu, J., Qian, Y., 2021. A cooperative-control-based underwater target escorting mechanism with multiple autonomous underwater vehicles for underwater internet of things. IEEE Internet of Things Journal 8, 4403–4416. doi:10.1109/JIOT.2020.3026355.

Zhang, Z., Wu, Y., 2021. Adaptive fuzzy tracking control of autonomous underwater vehicles with output constraints. IEEE Transactions on Fuzzy Systems 29, 1311–1319. doi:10.1109/TFUZZ.2020.2967294.

Zhao, C., Guo, L., 2020. Control of nonlinear uncertain systems by extended pid. IEEE Transactions on Automatic Control , 1–1doi:10.1109/TAC.2020.3030876.

Zheng, X., Wang, W., Xiong, M., Xie, G., 2020. Online state estimation of a fin-actuated underwater robot using artificial lateral line system. IEEE Transactions on Robotics 36, 472–487. doi:10.1109/TRO.2019.2956343.

Zhou, D., Li, Q., 2014. Indirect robust control of agile missile via theta-d technique. Defence Technology 10, 269–278.

Zhou, H., Wei, Z., Zeng, Z., Yu, C., Yao, B., Lian, L., 2020. Adaptive robust sliding mode control of autonomous underwater glider with input constraints for persistent virtual mooring. Applied Ocean Research 95, 102027.

Zhu, C., Huang, B., Zhou, B., Su, Y., Zhang, E., 2021. Adaptive model-parameter-free fault-tolerant trajectory tracking control for autonomous underwater vehicles. ISA transactions .

Zhu, D., Sun, B., 2013. The bio-inspired model based hybrid sliding-mode tracking control for unmanned underwater vehicles. Engineering applications of artificial intelligence 26, 2260–2269.

Auwal Shehu TIJJANI received the B.ENG. and M.ENG. degrees from the Bayero University, Kano, Nigeria and Univesiti Teknologi Malaysia, Johor Bahru, Malaysia, in 2012 and 2016, respectively. He is currently a PhD Student at the University of Montpellier Laboratory of Informatics, Robotics, and Microelectronics. His research interests include robust and adaptive control of autonomous underwater vehicles, AUVs.

Ahmed CHEMORI received the M.Sc. and Ph.D. degrees both in automatic control from the Grenoble Institute of Technology, Grenoble, France, in 2001 and 2005, respectively. He has been a Postdoctoral Fellow with the Automatic Control Laboratory, Grenoble, France, in 2006. He is currently a tenured Research Scientist in automatic control and robotics with LIRMM laboratory. His research interests include nonlinear adaptive, robust an predictive control and their applications in robotics.

Vincent CREUZE received his Ph.D. degree in 2002 from the University Montpellier 2 (France). He is currently Associate Professor with Accreditation to Supervise Research, at the University of Montpellier, attached to the Robotics Department of the LIRMM. His research interests include design, modelling, sensing and control, applied to underwater robots for deep archaeological applications or marine biology.